A perisinusoidal niche for extramedullary haematopoiesis in the spleen

Christopher N. Inra[#2], **Bo O. Zhou**[#2], **Melih Acar**[2], **Malea M. Murphy**[2], **James Richardson**[3], **Zhiyu Zhao**[2], and **Sean J. Morrison**[1,2,4]

[1]Howard Hughes Medical Institute, University of Texas Southwestern Medical Center, Dallas, Texas 75390, USA

[2]Department of Pediatrics and Children's Research Institute, University of Texas Southwestern Medical Center, Dallas, Texas 75390, USA

[3]Department of Pathology, University of Texas Southwestern Medical Center, Dallas, Texas 75390, USA

[#] These authors contributed equally to this work.

Abstract

Haematopoietic stresses mobilize haematopoietic stem cells (HSCs) from the bone marrow to the spleen and induce extramedullary haematopoiesis (EMH). However, the cellular nature of the EMH niche is unknown. Here, we assessed the sources of the key niche factors, SCF and CXCL12, in the mouse spleen after EMH induction by myeloablation, blood loss, or pregnancy. In each case, *Scf* was expressed by endothelial cells and *Tcf21*^{+} stromal cells, primarily around sinusoids in the red pulp, while *Cxcl12* was expressed by a subset of *Tcf21*^{+} stromal cells. EMH induction markedly expanded the *Scf*-expressing endothelial cells and stromal cells by inducing proliferation. Most splenic HSCs were adjacent to *Tcf21*^{+} stromal cells in red pulp. Conditional deletion of *Scf* from spleen endothelial cells or *Scf* or *Cxcl12* from *Tcf21*^{+} stromal cells severely reduced spleen EMH and reduced blood cell counts without affecting bone marrow haematopoiesis. Endothelial cells and *Tcf21*^{+} stromal cells thus create a perisinusoidal EMH niche in the spleen, which is necessary for the physiological response to diverse haematopoietic stresses.

The haematopoietic system employs facultative niches that arise in response to injury. Adult haematopoiesis occurs primarily in the bone marrow of mammals. However, a wide range of haematopoietic stresses including myelofibrosis[1], anaemia[2,3], pregnancy[4,5], infection[6,7],

[4]Correspondence: ; Email: Sean.Morrison@UTSouthwestern.edu

myeloablation[8], and myocardial infarction[9] can induce EMH, in which HSCs are mobilized to sites outside the bone marrow to expand haematopoiesis. The splenic red pulp is a prominent site of EMH in mice and humans[10-13]. During EMH, HSCs are found mainly around sinusoids in the red pulp, raising the possibility of a perisinusoidal niche[14]. CXCL12 is expressed by sinusoidal endothelial cells in the red pulp of the human spleen[15] and macrophage ablation reduces splenic erythropoiesis after irradiation[16]. However, little else is known about the EMH niche.

Niche factor expression in the spleen

HSCs are rare in normal adult spleen[17] but myeloablation with cyclophosphamide followed by daily administration of granulocyte colony-stimulating factor (G-CSF) induces HSC mobilization from the bone marrow to the spleen and induction of EMH[8]. Cyclophosphamide plus 21 days of G-CSF (Cy+21d G-CSF) increased erythropoiesis and myelopoiesis in the red pulp, profoundly increasing spleen size, spleen cellularity, HSC number, and progenitor numbers relative to control spleens (Extended Data Fig. 1c, 1f-1m).

In normal adult spleens from *Scf^GFP; Cxcl12^DsRed* mice[18,19], and after EMH induction, *Scf*-GFP and *Cxcl12*-DsRed were primarily expressed throughout the red pulp (Fig. 1a, 1b and Extended Data Fig 1a-1e). Red pulp endothelial cells and perivascular stromal cells expressed high levels of *Scf*-GFP, irrespective of EMH induction (Fig. 1a-1c and Extended Data Fig. 1d, 1e). In white pulp, *Scf*-GFP was expressed by many fewer stromal cells and central arteriolar endothelial cells (Fig. 1b and Extended Data Fig. 1e). *Cxcl12*-DsRed was not expressed by endothelial cells but was expressed by a subset of *Scf*-GFP$^+$ perivascular stromal cells, primarily around red pulp sinusoids and to a lesser extent around white pulp central arterioles (Fig. 1a-1c and Extended Data Fig. 1d, 1e).

Scf-GFP$^+$ cells were 0.48±0.10% of enzymatically dissociated adult spleen cells (Fig. 1d) and *Cxcl12*-DsRed$^+$ were 0.031±0.011% (Fig. 1f). Most *Scf*-GFP$^+$ cells (75±5.8%) were VE-cadherin$^+$CD45$^-$Ter119$^-$ endothelial cells (Fig. 1d): 85±8.2% of all VE-cadherin$^+$CD45$^-$Ter119$^-$ spleen endothelial cells were *Scf*-GFP$^+$ and none expressed *Cxcl12*-DsRed (Fig. 1e). Non-endothelial *Scf*-GFP$^+$ cells were virtually all PDGFRβ$^+$CD45$^-$Ter119$^-$ stromal cells (Fig. 1d). Some *Scf*-GFP$^+$ stromal cells (22±3.8%) also expressed *Cxcl12*-DsRed (Fig. 1d). Virtually all *Cxcl12*-DsRed$^+$ stromal cells expressed *Scf*-GFP (Fig. 1f). Therefore, *Scf* was expressed by VE-cadherin$^+$ endothelial cells and PDGFRβ$^+$ stromal cells while *Cxcl12* was expressed by a minority of *Scf*-expressing stromal cells in adult spleen.

EMH induction did not appear to alter spleen *Scf*-GFP or *Cxcl12*-DsRed expression (Fig. 1a versus Extended Data Fig. 1d). Flow cytometric analysis showed no change in the fluorescence intensity of individual *Scf*-GFP$^+$ or *Cxcl12*-DsRed$^+$ spleen cells after EMH induction (Extended Data Fig. 1o and 1p). However, the frequencies and absolute numbers of *Scf*-GFP and *Cxcl12*-DsRed cells increased significantly upon EMH induction (Fig. 1g-1j, Extended Data Fig. 1q and 1r). These cells rarely divided in normal adult spleen but proliferated upon EMH induction (Fig. 1k and 1j).

LepR$^+$ stromal cells are the main sources of *Scf* and *Cxcl12* for HSC maintenance in the bone marrow[18-20]. In the spleens of *Lepr*^{cre}; *R26*^{tdTomato} mice, recombination occurred mainly in the white pulp where HSCs are not observed[14] (Extended Data Fig. 1s). Only about 20% of *Scf*-GFP$^+$ stromal cells expressed LepR (Extended Data Fig. 1t). LepR$^+$ cells were PDGFRβ$^+$VE-cadherin$^-$ stromal cells that accounted for 37±13% of CFU-F formed by enzymatically dissociated spleen cells (Extended Data Fig. 1u and 1v).

Consistent with our prior study[19], *Lepr*^{cre}; *Scf*$^{fl/-}$ mice had significantly fewer CD150$^+$CD48$^-$LSK HSCs in the bone marrow and significantly increased spleen cellularity relative to *Scf*$^{+/-}$ and *Scf*$^{+/+}$ controls (Extended Data Fig. 1w and 1x). Upon EMH induction by Cy+4d G-CSF, *Lepr*^{cre}; *Scf*$^{fl/-}$ mice exhibited significant declines in spleen cellularity and spleen HSC number relative to controls (Extended Data Fig. 1x and 1y). While LepR$^+$ perivascular stromal cells could contribute to the EMH niche in adult spleen, the impaired EMH in these mice may also reflect bone marrow HSC depletion prior to EMH induction (Extended Data Fig. 1w).

Tcf21$^+$ perisinusoidal stromal cells express *Scf*

To identify Cre alleles that recombine in spleen, but not bone marrow, stromal cells we assessed the gene expression profile of spleen *Scf*-GFP$^+$VE-cadherin$^-$ stromal cells (Extended Data Table 1). After testing a number of Cre alleles (see Extended Data Fig. 2), we found that *Tcf21*-Cre/ER[21] recombined efficiently in spleen *Scf*-GFP$^+$ stromal cells (Fig. 2a) but not in bone marrow (Fig. 2b and 2c). *Tcf21*$^{cre/ER}$; *R26*^{tdTomato} mice gavaged with tamoxifen for 12 days at 4-6 weeks of age expressed Tomato in *Scf*-GFP$^+$ stromal cells throughout red pulp (Fig. 2a and 2d) but only in rare white pulp cells (Fig. 2a) and not in endothelial cells (Fig. 2d and 2e). Tomato$^+$CD45$^-$Ter119$^-$ stromal cells from enzymatically dissociated *Tcf21*$^{cre/ER}$; *R26*^{tdTomato} spleens accounted for 0.085±0.045% of spleen cells and 69±2% of spleen CFU-F (Fig. 2f and 2g). These cells were PDGFRβ$^+$ and LepR negative (Fig. 2f).

In the liver, *Scf*-GFP was exclusively expressed by VE-cadherin$^+$ endothelial cells (Extended Data Fig. 2a and 2b). *Tcf21*-Cre/ER recombined in 0.09% of liver cells, none of which expressed *Scf*-GFP (Extended Data Fig. 2a and 2c). The *Tcf21*-Cre/ER recombination pattern did not significantly change in the spleen (Fig. 2f and Extended Data Fig. 2d, 2e), bone marrow (Extended Data Fig. 2f and 2g), or liver (Extended Data Fig.2h and 2i) upon EMH induction by Cy+21d G-CSF.

c-kit$^+$ haematopoietic progenitors were almost exclusively within the red pulp in the normal spleen (Extended Data Fig. 3a and 3b) and after EMH induction (Fig. 2k). To assess HSCs localization we used a new technique that permits deep-imaging of *α-catulin*-GFP$^+$c-kit$^+$ HSCs in optically cleared haematopoietic tissues[22]. In the spleens of mice treated with Cy +4d G-CSF, only 0.019±0.01% of splenocytes were *α-catulin*-GFP$^+$c-kit$^+$ (Fig. 2h). All long-term multilineage reconstituting cells in the spleen were *α-catulin*-GFP$^+$ and 28% of *α-catulin*-GFP$^+$c-kit$^+$ spleen cells gave long-term multilineage reconstitution in primary (Fig. 2i) and secondary irradiated recipient mice (data not shown).

After antibody staining of a large segment of $Tcf21^{cre/ER}$; $R26^{tdTomato}$; α-$catulin^{GFP}$ spleen, we cleared the tissue (Extended Data Fig. 3c and 3d) then imaged to a depth of 300 μm and digitally reconstructed the tissue (Extended Data Fig. 3e, 3f and Supplementary video 1). α-catulin-GFP[+]c-kit[+] HSCs were found exclusively within the red pulp, where 80% were within 5μm of Tomato^{+} stromal cells (Fig. 2j).

EMH requires SCF and CXCL12 from *Tcf21^{+}* cells

To test if *Tcf21*-Cre/ER-expressing perivascular cells promote EMH, we treated 4-6-week-old $Tcf21^{cre/ER}$; $Scf^{fl/fl}$ and littermate control mice with tamoxifen for 12 days. A month later, bone marrow and spleen cellularity, blood cell counts, and bone marrow haematopoiesis were similar in $Tcf21^{cre/ER}$; $Scf^{fl/fl}$ mice and littermate controls (Fig. 3a-3f and Extended Data Fig. 3g-3l). Then we treated $Tcf21^{cre/ER}$; $Scf^{fl/fl}$ mice and littermate controls with cyclophosphamide followed by 4, 8, or 21 days of G-CSF. $Tcf21^{cre/ER}$; $Scf^{fl/fl}$ mice did not differ from controls with respect to bone marrow cellularity (Fig. 3a) or the numbers of HSCs (Fig. 3b), common myeloid progenitors (CMPs[23]), granulocyte-monocyte progenitors (GMPs[23]), or megakaryocyte-erythroid progenitors (MEPs[23]) in the bone marrow after Cy+G-CSF treatment (Extended Data Fig. 3j-3l). In contrast, $Tcf21^{cre/ER}$; $Scf^{fl/fl}$ mice had significantly fewer splenocytes (Fig. 3c), spleen HSCs (Fig. 3d), CMPs (Fig. 3e), GMPs (Extended Data Fig. 3m) and MEPs (Fig. 3f) relative to littermate controls after 8 to 21 days of G-CSF treatment. We did not detect any difference between $Tcf21^{cre/ER}$; $Scf^{fl/fl}$ mice and littermate controls in terms of vascular or stromal cell morphology in the spleen, with or without induction of EMH (Extended Data Fig. 4a-4g). Conditional deletion of *Scf* with *Tcf21*-Cre/ER thus depletes HSCs and reduces EMH in the spleen without affecting bone marrow haematopoiesis.

Red (RBC) and white blood cell (WBC) counts were significantly lower in $Tcf21^{cre/ER}$; $Scf^{fl/fl}$ mice as compared to controls after 8 to 21 days of G-CSF treatment (Extended Data Fig. 3g-3i). Splenectomy significantly reduced RBC and WBC counts in mice treated with Cy+G-CSF, demonstrating that splenic EMH is necessary for the recovery of blood cell counts (Fig. 3g, 3h and Extended Data Fig. 3n). However, conditional deletion of *Scf* by *Tcf21*-Cre/ER did not further reduce blood cell counts in splenectomized mice (Fig. 3g and 3h). SCF expression by *Tcf21^{+}* stromal cells in the spleen is thus necessary for the regeneration of blood cells after Cy+G-CSF treatment.

Bone marrow cellularity and bone marrow haematopoiesis were similar in $Tcf21^{cre/ER}$; $Cxcl12^{fl/-}$ mice and littermate controls, before and after Cy+G-CSF treatment (Fig. 3i, 3j and Extended Data Fig. 3r-3t). However, $Tcf21^{cre/ER}$; $Cxcl12^{fl/-}$ mice exhibited significantly reduced spleen cellularity (Fig. 3k) and numbers of spleen CMPs, GMPs, and MEPs (Fig. 3m, 3n and Extended Data Fig. 3u) relative to controls after 8 to 21 days of G-CSF treatment. Although the number of HSCs in the spleens of $Tcf21^{cre/ER}$; $Cxcl12^{fl/-}$ mice did not significantly differ from littermate controls (Fig. 3l), HSC numbers were significantly elevated in the blood (Fig. 3o) and in the bone marrow (Fig. 3j) of $Tcf21^{cre/ER}$; $Cxcl12^{fl/-}$ mice after 21 days of G-CSF treatment. This suggests that some HSCs were mobilized from the spleens of $Tcf21^{cre/ER}$; $Cxcl12^{fl/-}$ mice. $Tcf21^{cre/ER}$; $Cxcl12^{fl/-}$ mice also had significantly reduced RBC counts after 21 days of G-CSF treatment (Extended Data Fig.

3o-3q). We did not detect any difference between $Tcf21^{cre/ER}$; $Cxcl12^{fl/-}$ mice and littermate controls in terms of the frequency or morphology of vascular or stromal cells in the spleen, with or without EMH (Extended Data Fig. 4h-4n). $Tcf21$-Cre/ER-expressing stromal cells are thus an important source of CXCL12 for spleen EMH but not bone marrow haematopoiesis.

EMH requires SCF from endothelial cells

We discovered that $Vav1$-cre recombines efficiently in spleen, but not bone marrow, endothelial cells. $Vav1$-cre; $R26^{tdTomato}$ mice recombined throughout the red pulp in VE-cadherin$^+$$Scf$-GFP$^+$ cells but only in rare white pulp cells (Fig. 4a-4c). VE-cadherin$^+$$Scf$-GFP$^+$ cells accounted for 0.37±0.07% of enzymatically dissociated spleen cells and 83±5.3% of these cells recombined with $Vav1$-cre (Fig. 4b). These cells were negative for PDGFRβ (Extended Data Fig. 5a). 70±5% of VE-cadherin$^+$ endothelial cells were Tomato$^+$ in the spleens of $Vav1$-cre; $R26^{tdTomato}$ mice but only 8.4±0.5% were Tomato$^+$ in bone marrow (Extended Fig. 5b, 5e-5h). Endothelial cells from $Vav1$-cre; $Scf^{fl/-}$ mice exhibited a 6.5-fold reduction in Scf transcript levels (Extended Data Fig. 5c) and a 5.6-fold reduction in SCF protein (Extended Data Fig. 5d) relative to endothelial cells from $Scf^{fl/-}$ controls.

In the livers of $Vav1$-cre; $R26^{tdTomato}$; Scf^{GFP} mice recombination occurred in 26±4.2% of VE-cadherin$^+$$Scf$-GFP$^+$ cells (Extended Data Fig. 5i-5k). Upon induction of EMH by Cy +G-CSF, $Vav1$-Cre recombination did not significantly change in the spleen (Extended Data Fig. 5b, 6a and 6b), bone marrow (Extended Data Fig. 5b, 6c and 6d), or liver (Extended Data Fig. 6e and 6f).

$Cxcl12$ was not expressed by spleen endothelial cells (Fig. 1e). Consistent with this, $Vav1$-cre; $Cxcl12^{fl/-}$ mice had normal blood counts, cellularity, and numbers of HSCs, CMPs, GMPs, and MEPs in bone marrow and spleen after Cy+G-CSF (Extended Data Fig. 6g-6s).

$Vav1$-Cre also recombines in haematopoietic cells[24] but haematopoietic cells do not express Scf and $Vav1$-cre; $Scf^{fl/-}$ mice have normal HSC frequency and haematopoiesis in bone marrow[18,19]. Prior to EMH induction with Cy+G-CSF, $Vav1$-cre; $Scf^{fl/-}$ mice did not significantly differ from $Scf^{fl/-}$ controls with respect to bone marrow or spleen cellularity, or the numbers of HSCs, CMPs, GMPs, or MEPs in the bone marrow or spleen (Fig. 4d-4i and Extended Data Fig. 6w-6z). After Cy+G-CSF treatment, bone marrow cellularity and numbers of bone marrow HSCs, CMPs, GMPs, or MEPs in $Vav1$-cre; $Scf^{fl/-}$ mice were normal (Fig. 4d, 4e and Extended Data Fig. 6w-6y). However, RBC counts, spleen cellularity, and the numbers of spleen HSCs, CMPs, and MEPs declined in $Vav1$-cre; $Scf^{fl/-}$ mice relative to $Scf^{fl/-}$ controls (Fig. 4f-4i; Extended Data Fig. 6t-6v).

The decline in blood cell counts in $Vav1$-cre; $Scf^{fl/-}$ mice after EMH induction was caused by reduced spleen EMH because splenectomy significantly reduced RBC and WBC counts but conditional deletion of Scf in splenectomized $Vav1$-cre; $Scf^{fl/-}$ mice had no further effect on blood cell counts (Fig. 4j and 4k). We did not detect any difference between $Vav1$-cre; $Scf^{fl/-}$ mice and controls in terms of the frequency or morphology of vascular or stromal

cells in the spleen (Extended Data Fig. 4o-4u). Endothelial *Scf* expression is thus necessary for splenic EMH and the recovery of blood cell counts after Cy+G-CSF.

The splenic EMH niche during pregnancy

Erythropoiesis and myelopoiesis significantly increased in the red pulp during pregnancy, profoundly increasing spleen cellularity, HSC number, and progenitor numbers relative to non-pregnant mice (Extended Data Fig. 7a-7i). Just as in Cy+G-CSF-treated mice, *Scf*-GFP was largely expressed by endothelial and perivascular stromal cells in the red pulp and *Cxcl12*-DsRed was expressed by a subset of the *Scf*-GFP$^+$ stromal cells (Extended Data Fig. 7j-7l). Pregnancy induced these cells to proliferate, significantly expanding their numbers (Extended Data Fig. 7m-7o). In pregnant mice, *Tcf21*-Cre/ER recombined in spleen PDGFRβ$^+$LepR$^-$ stromal cells but not in bone marrow and rarely in liver (Extended Data Fig. 7p-7v). *Vav1-cre, Scf*$^{fl/fl}$ mice were infertile, preventing us from testing the endothelial contribution to EMH during pregnancy.

Pregnant *Tcf21*$^{cre/ER}$; *Scf*$^{fl/fl}$ females did not differ from *Scf*$^{fl/fl}$ control females in terms of bone marrow cellularity (Fig. 5a), or the numbers of HSCs (Fig. 5b), GMPs, CMPs, or MEPs in the bone marrow (Extended Data Fig. 8a-8d). In contrast, pregnant *Tcf21*$^{cre/ER}$; *Scf*$^{fl/fl}$ females exhibited significantly lower spleen cellularity and numbers of HSCs, GMPs, CMPs, MEPs, myeloid and erythroid cells in the spleen as compared to pregnant *Scf*$^{fl/fl}$ females (Fig. 5c-5f and Extended Data Fig. 8e, 8f). Pregnant *Tcf21*$^{cre/ER}$; *Scf*$^{fl/fl}$ females had significantly lower RBC counts than pregnant *Scf*$^{fl/fl}$ controls (Fig. 5g), and significantly lower fetal mass (Fig. 5h). SCF from *Tcf21*$^+$ perivascular cells is thus necessary for splenic EMH and for the expansion of erythropoiesis during pregnancy.

Pregnant *Tcf21*$^{cre/ER}$; *Cxcl12*$^{fl/-}$ females also had significantly reduced splenic cellularity and splenic erythropoiesis relative to pregnant *Cxcl12*$^{fl/-}$ controls, without any changes in bone marrow haematopoiesis (Extended Data Fig. 8i-8x).

The splenic EMH niche after blood loss

Repeated bleeding significantly increased erythropoiesis and myelopoiesis in the red pulp, increasing spleen cellularity, HSC number, and progenitor numbers relative to non-bled controls (Extended Data Fig. 9a-9i). Just as in Cy+G-CSF-treated mice, *Scf*-GFP was largely expressed by endothelial cells and perivascular stromal cells in the red pulp while *Cxcl12*-DsRed was expressed by a subset of *Scf*-GFP$^+$ stromal cells (Extended Data Fig. 9j-9l). Blood loss induced the proliferation of these cells, significantly expanding their numbers (Extended Data Fig. 9m-9o). In bled mice, *Tcf21*-Cre/ER recombined in red pulp PDGFRβ$^+$LepR$^-$ stromal cells, but not in bone marrow and rarely in liver (Extended Data Fig. 9p-9v). *Vav1*-Cre recombined in 66±4.2% of spleen endothelial cells, mainly in the red pulp, but only in 7.5±4.0% of bone marrow endothelial cells and 25±5.8% of liver endothelial cells (Extended Data Fig. 10a-10h).

Bled *Tcf21*$^{cre/ER}$; *Scf*$^{fl/fl}$ mice or *Vav1-cre*; *Scf*$^{fl/fl}$ mice did not differ from bled *Scf*$^{fl/fl}$ controls in bone marrow cellularity (Fig. 5i), or the numbers of HSCs (Fig. 5j), GMPs, CMPs, or MEPs in the bone marrow (Extended Data Fig. 10i-10l). In contrast, bled

Tcf21$^{cre/ER}$; Scf$^{fl/fl}$ mice and *Vav1-cre; Scf$^{fl/fl}$* mice each had significantly lower RBC counts, spleen cellularity, and numbers of HSCs, GMPs, CMPs, MEPs, myeloid and erythroid cells in the spleen as compared to bled *Scf$^{fl/fl}$* controls (Fig. 5l-5o and Extended Data Fig. 10m-10p). *Tcf21^{+}* stromal cells and endothelial cells are thus necessary for EMH in the spleen and for the expansion of erythropoiesis after bleeding.

Endothelial and *Tcf21^{+}* stromal cells had additive effects on splenic EMH and the recovery of RBC counts after bleeding. Bled *Vav1-cre; Tcf21$^{cre/ER}$; Scf$^{fl/fl}$* mice had similar bone marrow cellularity and numbers of HSCs in the bone marrow as bled *Scf$^{fl/fl}$* controls (Fig. 5i and 5j). However, they had significantly reduced RBC counts, spleen cellularity, and numbers of HSCs, MEPs, and erythroid cells in the spleen as compared to bled *Scf$^{fl/fl}$* mice, bled *Vav1-cre; Scf$^{fl/fl}$* mice, and bled *Tcf21$^{cre/ER}$; Scf$^{fl/fl}$* mice (Fig. 5k-5n and Extended Data Fig. 10p).

Bled *Tcf21$^{cre/ER}$; Cxcl12$^{fl/-}$* mice also had significantly reduced cellularity, MEPs, and erythroid cells in the spleen as well as significantly reduced RBC counts as compared to bled *Cxcl12$^{fl/-}$* controls, without any differences in bone marrow haematopoiesis (Extended Data Fig. 10q-10ae).

The EMH niche in mouse spleen is created by endothelial cells and *Tcf21*-expressing stromal cells associated with red pulp sinusoids and is functionally important for haematopoietic recovery from a range of stresses. A prior study[15] detected CXCL12 expression in endothelial cells in human spleens. This suggests that endothelial cells are also a component of the EMH niche in humans but there may be species differences in CXCL12 expression among niche cells. It is not clear whether there is any relationship between the *Cxcl12*-abundant reticular (CAR) cells that are part of the bone marrow niche[25] and the *Cxcl12*-expressing stromal cells in the splenic EMH niche. While bone marrow CAR cells are LepR^{+} and *Tcf21* negative, spleen CAR cells are *Tcf21^{+}* and LepR negative.

METHODS

Mice

All mice were maintained on a C57BL/6 background, including *Scf^{GFP}*[19], *Scf$^{fl/+}$*[19], *Cxcl12^{DsRed}*[18], *Cxcl12$^{fl/+}$*[18], *R26^{tdTomato}*[26], *Vav1-cre*[24], *Lepr^{cre}*[27], *Tcf21$^{cre/ER}$*[21] and *α-catulin^{GFP}*. To induce CreER activity in *Tcf21$^{cre/ER}$* mice, 4-6-week-old mice were administered 2 mg tamoxifen (Sigma) daily by oral gavage for 12 consecutive days. For induction of EMH, mice were injected at day 0 with a single dose of 4 mg cyclophosphamide followed by daily injections of 5 µg G-CSF for 4 to 21 days. Both male and female mice were used. All mice were housed in the Animal Resource Center at the University of Texas Southwestern Medical Center (UTSW). All procedures were approved by the UTSW Institutional Animal Care and Use Committee.

Flow cytometric analysis of haematopoietic cells

Bone marrow cells were isolated by flushing the femur or tibia with Ca^{2+} and Mg^{2+} free HBSS with 2% heat-inactivated bovine serum using a 3 ml syringe fitted with a 25-gauge needle. Spleen cells were obtained by crushing the spleen between two frosted slides. The

cells were dissociated to a single cell suspension by gently passing through the needle several times and then filtering through a 40 μm nylon mesh. Blood was collected by cardiac puncture, and white blood cells were isolated by ficoll centrifugation according to the manufacturer's instructions (GE Healthcare). The following antibodies were used to isolate HSCs: anti-CD150 (TC15-12F12.2), anti-CD48 (HM48-1), anti-Sca-1 (E13-161.7), anti-c-kit (2B8) and the following antibodies against lineage markers (anti-Ter119, anti-B220 (6B2), anti-Gr1 (8C5), anti-CD2 (RM2-5), anti-CD3 (17A2), anti-CD5 (53-7.3) and anti-CD8 (53-6.7)). Haematopoietic progenitors were identified by flow cytometry using the following antibodies: anti-Sca-1 (E13-161.7), anti-c-kit (2B8) and the following antibodies against lineage markers (anti-Ter119, anti-B220 (6B2), anti-Gr1 (8C5), anti-CD2 (RM2-5), anti-CD3 (17A2), anti-CD5 (53-7.3) and anti-CD8 (53-6.7)), anti-CD34 (RAM34), anti-CD135 (Flt3) (A2F10), anti-CD16/32 (FcγR) (93), anti-CD127 (IL7Rα) (A7R34), anti-CD24 (M1/69), anti-CD43 (1B11), anti-B220 (6B2), anti-IgM (II/41), anti-CD3 (17A2), anti-Gr-1 (8C5), anti-Mac-1 (M1/70), anti-CD41 (MWReg30), anti-CD71 (C2) and anti-Ter119. DAPI was used to exclude dead cells. Antibodies were obtained from eBioscience or BD Bioscience.

Flow cytometric analysis of stromal cells

To isolate bone marrow stromal cells the marrow was gently flushed out of the bone marrow cavity with a 3-ml syringe fitted with a 23-guage needle and then transferred into 1 ml pre-warmed bone marrow digestion solution (200 U/ml DNase I (Sigma), 250 μg/ml Liberase^{DL} (Roche) in HBSS plus Ca^{2+} and Mg^{2+}) and incubated at 37°C for 30 minutes with gentle shaking. To isolate splenic stromal cells, the spleen capsule was cut into ~1 mm^3 fragments using scissors and then digested as above in spleen digestion solution (200 U/ml DNase I, 250 μg/ml Liberase^{DL}, 1 mg/ml Collagenase, type 4 (Roche) and 500 μg/ml Collagenase D (Roche) in HBSS plus Ca^{2+} and Mg^{2+}). After a brief vortex, the spleen fragments were allowed to sediment for ~3 minutes and the supernatant was transferred to another tube on ice. The sedimented (undigested) spleen fragments were subjected to a second round of digestion. The two fractions of digested cells were pooled and filtered through a 100 μm nylon mesh. Anti-PDGFRα (APA5), anti-PDGFRβ (APB5), anti-LepR (R&D), anti-CD45 (30F-11) and anti-Ter119 antibodies were used to isolate stromal cells. For analysis of endothelial cells, mice were injected intravenously into the retro-orbital venous sinus with 10 μg Alexa Fluor 660 conjugated anti-VE-cadherin antibody (BV13) 10 minutes before sacrifice. Samples were analyzed using a FACSAria or FACSCanto II flow cytometer (BD Biosciences).

5-bromo-2′-deoxyuridine (BrdU) incorporation assay

To assess BrdU incorporation into spleen cells after EMH induction, mice were intraperitoneally injected with a single dose of BrdU (2mg BrdU/per mouse) then maintained on 0.5mg BrdU/ml drinking water for seven days. Endothelial cells were labeled by intravenous injection of an anti-VE-cadherin antibody (eBioscience). Enzymatically dissociated spleen cells were stained with antibodies against surface markers and the target cell populations were sorted then resorted to ensure purity. The sorted cells were then fixed, and stained with an anti-BrdU antibody using the BrdU APC Flow Kit (BD Biosciences) according to the manufacturer's instructions.

Long-term competitive reconstitution assay

Adult recipient mice were irradiated using an XRAD 320 x-ray irradiator (Precision X-Ray Inc.) with two doses of 540 rad (total 1080 rad) delivered at least 2 hours apart. Cells were injected into the retro-orbital venous sinus of anesthetized mice. Sorted doses of splenocytes from donor mice with EMH were transplanted along with 3×10^5 recipient bone marrow cells. Recipient mice were bled every 4 weeks to assess the level of donor-derived blood cells, including myeloid, B and T cells for at least 16 weeks. Blood was subjected to ammonium chloride/potassium red cell lysis before antibody staining. Antibodies including anti-CD45.2 (104), anti-CD45.1 (A20), anti-Gr1 (8C5), anti-Mac-1 (M1/70), anti-B220 (6B2), and anti-CD3 (KT31.1) were used for flow cytometric analysis.

Tissue sectioning and confocal imaging

For bone marrow sections, freshly dissected bones were fixed in 4% paraformaldehyde overnight followed by 3 days of decalcification in 10% EDTA dissolved in PBS. Bones were sectioned using the CryoJane tape-transfer system (Instrumedics). For spleen sections, freshly dissected spleens were fixed in 4% paraformaldehyde for 1 hour followed by 1 day incubation in 10% Sucrose in PBS. Frozen spleens were sectioned with a cryostat (Leica). For whole mount imaging, spleens were sectioned into ~2 mm pieces. Spleen sections were blocked in PBS with 10% horse serum for 1 hour and then stained overnight with chicken-anti-GFP (Aves), and/or rabbit-anti-Laminin (Abcam) antibodies. Donkey-anti-chicken Alexa Fluor 488 and/or Donkey-anti-rabbit Alexa Fluor 647 were used as secondary antibodies (Invitrogen). Specimens were mounted with anti-fade prolong gold (Invitrogen) and images were acquired with either a Zeiss LSM780 confocal microscope or a Leica SP8 confocal microscope equipped with a resonant scanner. Three dimensional images were achieved using Bitplane Imaris v7.7.1 software.

Deep imaging of spleens

Spleens were harvested and fixed for 4 hours in 4% PFA at 4°C. Since the Spleen capsule is highly autofluorescent, spleens were sectioned perpendicular to the long axis into 300 μm thick sections using a Leica VT100S vibratome. These 300 μm sections were fixed for an additional 2 hours in 4% PFA and blocked overnight in staining solution (10% DMSO, 0.5% IgePal630 (Sigma), and 5% donkey serum (Jackson Immunoresearch) in PBS). All staining steps were performed in staining solution on a rotator at room temperature. Spleen sections were stained for three days in primary antibodies, washed overnight in several changes of PBS then stained for three days in secondary antibodies. The stained sections were dehydrated in a methanol dehydration series then incubated for 3 hours in 100% methanol with several changes. The methanol was then exchanged with benzyl alcohol:benzyl benzoate 1:2 mix (BABB clearing[28]). The tissues were incubated in BABB for 3 hours to overnight with several exchanges of fresh BABB. Spleen sections were mounted in BABB between two cover slips and sealed with silicone (Premium waterproof silicone II clear, General Electric). We found it necessary to clean the BABB of peroxides (which can accumulate as a result of exposure to air and light) by adding 10 g of activated aluminum oxide (Sigma) to 40ml of BABB and rotating for at least 1 hour, then centrifuging at 2000×g for 10 minutes to remove the suspended aluminum oxide particles. Images were acquired

using a Zeiss LSM780 confocal microscope with a Zeiss LD LCI Plan-Apo 25×/0.8 multi-immersion objective lens, which has a 570 μm working distance. Images were taken at 512×512 pixel resolution with 2 μm Z-steps, pinhole for the internal detector at 47.7 μm. Random spots were inserted into images by generating randomized X, Y, and Z coordinates using the random integer generator at www.random.org.

Splenectomy

After mouse anesthesia by Ketamine/xylazine, a ventral midline incision was made and the peritoneum was breached. The splenic blood vessels was ligated with an absorbable suture (4-0 vicryl). The splenic vessels was cut distal to the suture and the spleen was removed. The vessels was cauterized and the abdomen was sutured with non-absorbable sutures (3-0 Tevdek III). Buprenorphine was administered every 12 hours for 3 days to minimize postoperative pain and mice were maintained with ampicillin-containing water to avoid infection. Complete blood counts were measured one month after the survival surgery.

Induction of EMH by bleeding

EMH was induced by repeated bleeding over a two week period according to a published protocol[2]. Briefly, 4-6 month-old mice were bled via the tail-vein five times, every three days, removing approximately 250 μl of blood each time, then the mice were sacrificed for analysis two days after the last bleed.

Western blot

Approximately 30,000 CD45$^-$Ter119$^-$VE-cadherin$^+$ splenic endothelial cells were flow cytometrically sorted into 50 μl of 66% Trichoracetic acid (TCA) in water. Extracts were incubated on ice for at least 15 min and centrifuged at $16,100 \times g$ at 4°C for 10 min. Precipitates were washed in acetone twice and the dried pellets were solubilized in 9M urea, 2% TritonX-100, and 1% DTT. Samples were separated on 4-12% Bis-Tris polyacrylamide gels (Invitrogen) and transferred to PVDF membrane (Millipore). The blots were incubated with primary antibodies overnight at 4°C and then with secondary antibodies. Blots were developed with the SuperSignal West Femtochemiluminescence kit (Thermo Scientific). Primary antibodies used: rabbit-anti-SCF (Abcam, 1:1000) and mouse-anti-Actin (Santa Cruz, clone AC-15, 1:20,000).

Quantitative real-time PCR

Cells were sorted directly into Trizol (Life Technologies). Total RNA was extracted according to the manufacturer's instructions. Total RNA was reverse transcribed using SuperScript III Reverse Transcriptase (Life Technologies). Quantitative real-time PCR was performed using SYBR green on a LightCycler 480 (Roche). *β-actin* was used to normalize the RNA content of samples. Primers used in this study were *Scf*: 5'-GCCAGAAACTAGATCCTTTACTCCTGA-3' and 5'-CATAAATGGTTTTGTGACACTGACTCTG-3'; *β-actin*: 5'-GCTCTTTTCCAGCCTTCCTT-3' and 5'- CTTCTGCATCCTGTCAGCAA-3'.

Gene expression profiling

Three independent samples of 5,000 spleen *Scf*-GFP$^+$VE-cadherin$^-$ spleen stromal cells and two independent samples of 5,000 unfractionated spleen cells were flow cytometrically sorted into Trizol. Total RNA was extracted, amplified, and sense strand cDNA was generated using the Ovation Pico WTA System V2 (NuGEN) according to the manufacturer's instructions. cDNA was fragmented and biotinylated using the Encore Biotin Module (NuGEN) according to the manufacturer's instructions. Labeled cDNA was hybridized to Affymetrix Mouse Gene ST 1.0 chips according to the manufacturer's instructions. Expression values for all probes were normalized and determined using the robust multi-array average (RMA) method[29]. Microarray data are available at GEO database: http://www.ncbi.nlm.nih.gov/ (accession number GSE71288).

Statistical methods

Panels in all figures represented multiple independent experiments performed on different days with different mice. Sample sizes were not based on power calculations. No randomization or blinding was performed. No animals were excluded from analysis. Variation is always indicated using standard deviation. For analysis of the statistical significance of differences between two groups we generally performed two-tailed Student's *t*-tests. For analysis of the statistical significance of differences among more than two groups, we performed Repeated Measures one-way ANOVAs with Greenhouse-Geisser correction (variances between groups were not equal) and Tukey's multiple comparison tests with individual variances computed for each comparison. To assess the statistical significance of differences in fetal mass between paired control and mutant mice (Fig. 5j and Extended Data Fig. 8v), we performed a two-way ANOVA.
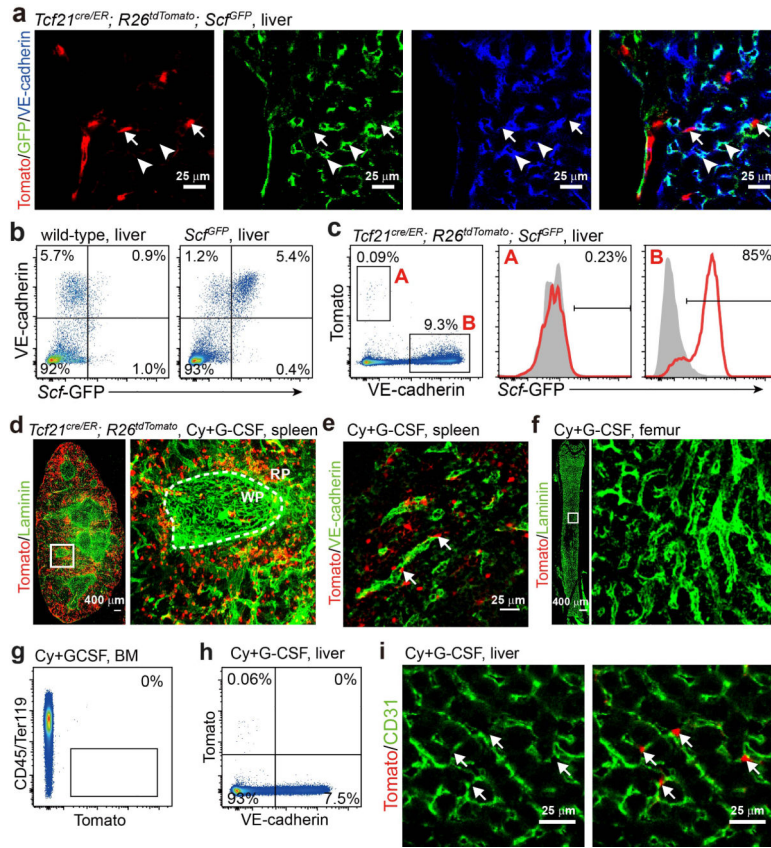
Extended Data
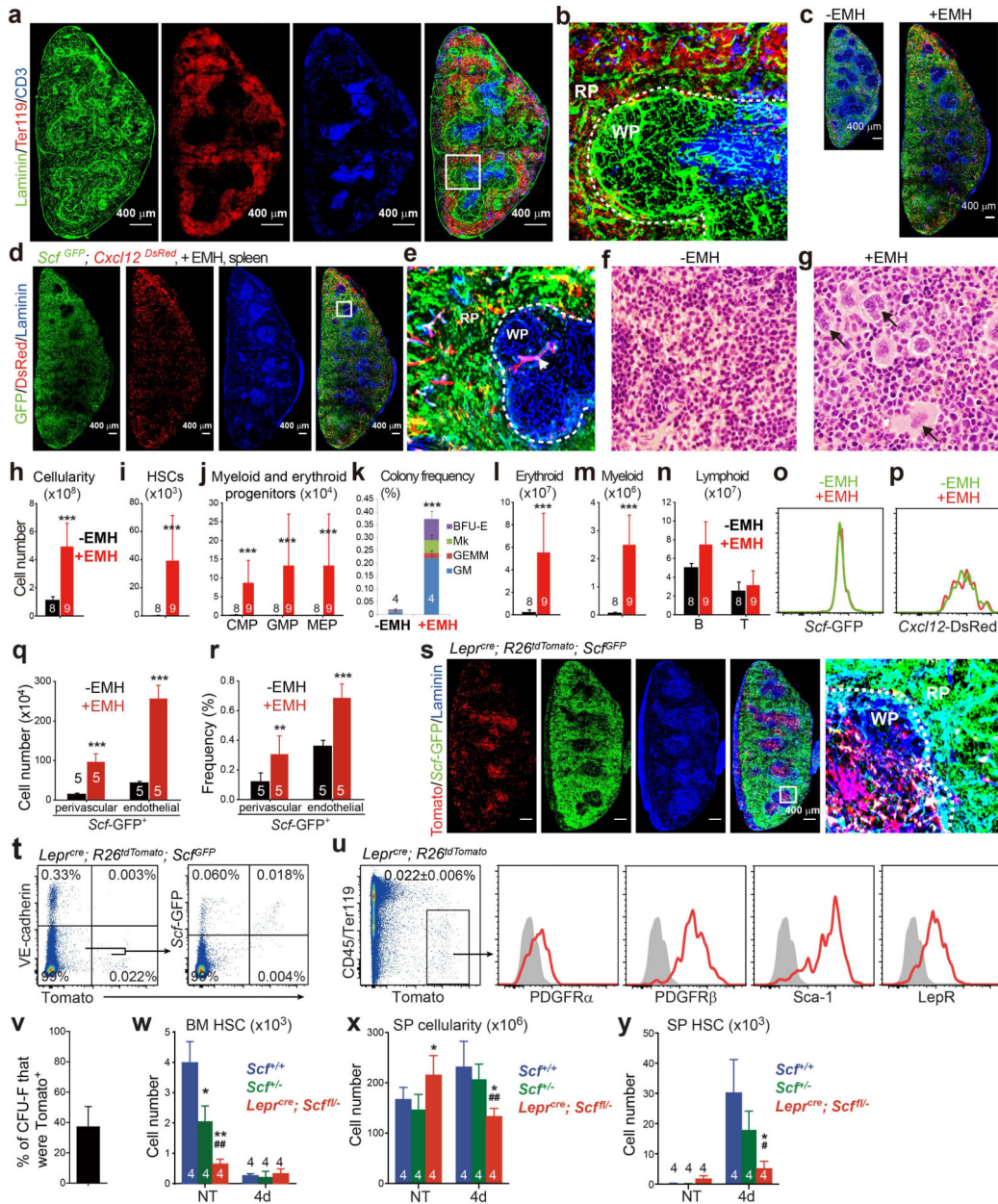
Extended Data Figure 1. Cy+21d G-CSF treatment induces EMH in the spleen and deletion of *Scf* from LepR⁺ cells significantly reduces the number of HSCs in the bone marrow and the spleen after induction of EMH

a, b, Staining with anti-Laminin antibody distinguished the vasculature of red pulp (RP) from white pulp (WP). The red pulp and white pulp were marked by clusters of Ter119⁺ cells (red) and CD3⁺ cells (blue), respectively[30]. Dashed line depicts the boundary between red pulp and white pulp. (representative images from 3 mice in 3 independent experiments). **c,** Spleen sections of the same magnification show the enlargement of the spleen after induction of EMH by Cy+21day G-CSF. These are the same images as in Fig. 1a and Extended Data Fig. 1d, adjusted to reflect the same magnification. **d, e,** Imaging of thick

spleen sections from Scf^{GFP}; $Cxcl12^{DsRed}$ mice after the induction of EMH by Cy+21d G-CSF. **e**, High-magnification view of the boxed area in (**d**). Dashed lines depict the boundaries between white pulp and red pulp. Arrow indicates the central arteriole in the white pulp around which stromal cells expressed $Cxcl12$-DsRed. (representative images from 3 mice from 3 independent experiments). **f, g,** Hematoxylin and Eosin (H&E) staining showing the increase in haematopoiesis in the spleen after induction of EMH using Cy+G-CSF (+EMH, **g**) as evidenced by the presence of megakaryocytes (arrows; n=3 mice/condition from 3 independent experiments). **h-n,** Cy+G-CSF treatment significantly increased spleen cellularity (**h**), as well as the numbers of HSCs (**i**), myeloid and erythroid progenitors (**j**), frequencies of colony-forming progenitors (**k**), numbers of Ter119$^+$ erythroid cells (**l**) and Gr-1$^+$Mac-1$^+$ myeloid cells (**m**) in the spleen but not the number of B220$^+$ or CD3$^+$ lymphoid cells (**n**). The numbers of mice per treatment are shown in each bar of each panel. Each panel shows mean±s.d. from five independent experiments. **o, p,** Scf-GFP (**o**) and $Cxcl12$-DsRed (**p**) fluorescence by spleen stromal cells before (–EMH) and after induction of EMH (+EMH) using Cy+G-CSF. **q, r,** The frequencies (**q**) and absolute numbers (**r**) of Scf-GFP$^+$VE-cadherin$^+$ endothelial cells and Scf-GFP$^+$VE-cadherin$^-$ stromal cells significantly increased upon induction of EMH by Cy+21d G-CSF (+EMH). **s,** Spleens from $Lepr^{cre}$; $R26^{tdTomato}$; Scf^{GFP} mice showed Tomato expression was primarily in the stromal cells of the white pulp. Although most Scf-GFP expression was in endothelial cells and perivascular stromal cells of the red pulp (Fig. 1a-1d), some Scf-GFP$^+$ stromal cells were in the white pulp, most of which appeared to express LepR. Dashed line depicts the boundary between red pulp (RP) and white pulp (WP). (representative images of 6 mice from 4 independent experiments). **t,** Flow cytometric analysis of enzymatically dissociated spleen cells from $Lepr^{cre}$; $R26^{tdTomato}$; Scf^{GFP} mice showed that only a small minority of non-endothelial Scf-GFP$^+$ cells were positive for Tomato (n=3 mice from 3 independent experiments). **u,** Tomato$^+$CD45$^-$Ter119$^-$ stromal cells in the spleens of $Lepr$-cre; $R26^{tdTomato}$ mice expressed PDGFRα, PDGFRβ, Sca-1, and LepR (n=3 mice from 3 independent experiments). **v,** Percentage of all CFU-F colonies formed by enzymatically dissociated spleen cells from $Lepr^{cre}$; $R26^{tdTomato}$ mice that expressed Tomato. Macrophage colonies were excluded by staining with anti-CD45 antibody (n=4 mice from 3 independent experiments). **w,** $Lepr^{cre}$; $Scf^{fl/-}$ mice had significantly fewer HSCs in the bone marrow than wild-type and $Scf^{fl/-}$ controls before induction of EMH (n=4 mice/genotype/time point mice from 4 independent experiments). **x, y,** $Lepr^{cre}$; $Scf^{fl/-}$ mice displayed significantly lower spleen cellularity (**x**) and HSC number (**y**) in the spleen than wild-type and $Scf^{fl/-}$ controls after induction of EMH with cyclophosphamide plus 4 days of G-CSF. The numbers of mice per treatement are shown in each bar. Data represent mean±s.d. from 4 independent experiments. The statistical significance of differences (**1h-1n, 1q and 1r**) was assessed using two-tailed Student's t-tests (*** $P<0.001$). The statistical significance of differences between genotypes (**1w-1y**) was assessed using Repeated Measures one-way ANOVAs with Greenhouse-Geisser correction and Tukey's multiple comparison tests with individual variances computed for each comparison. * indicates statistical significance relative to wild-type ($Scf^{+/+}$). # indicates statistical significance between $Scf^{+/-}$ and $Lepr^{cre}$; $Scf^{fl/-}$ (* or # $P<0.05$, ** or ## $P<0.01$).

Extended Data Figure 2. ***Scf*** **is expressed by most endothelial cells but not by** ***Tcf21*^{+} **perivascular cells in the liver; Cy+21d G-CSF does not significantly change the recombination pattern of** ***Tcf21*-Cre/ER in the spleen, bone marrow or liver**

To identify Cre alleles that recombine in spleen, but not bone marrow, stromal cells we assessed the gene expression profile of spleen *Scf*-GFP[+]VE-cadherin^{−} stromal cells (Extended Data Table 1). *Nestin*, *NG2* (*Cspg4*), and *Prx1* were low or undetectable (data not shown). *Nestin*-Cre[31], *NG2*-Cre[32], *NG2*-Cre/ER[33], and *Prx1*-Cre[34] did not recombine widely or specifically in *Scf*-GFP^{+} stromal cells in the spleen (data not shown). *Pdgfra* and *Pdgfrb* were expressed by spleen *Scf*-GFP^{+} stromal cells but neither *Pdgfra*-Cre/ER[35] nor *Pdgfrb*-Cre[36] recombined efficiently (data not shown). *Sm22* (*Tagln*), *Myh11*, *Sma* (*Acta2*), and *Tcf21* were significantly more highly expressed by spleen than bone marrow *Scf*-GFP^{+} stromal cells (Extended Data Table 1). *Sm22*-Cre[37], *Myh11*-Cre[38], and *Sma*-Cre/ER[39] recombined in few spleen *Scf*-GFP^{+} stromal cells (data not shown). However, *Tcf21*-Cre/ER recombined in perivascular stromal cells in the spleen but not bone marrow (Figure 2). **a-c,** Under normal conditions, *Scf*-GFP was expressed by most VE-cadherin^{+} endothelial cells (arrowheads in **a**) but not by *Tcf21*^{+} stromal cells (arrows in **a**) in the liver (n=3 mice from 3 independent experiments). **d, e,** EMH induced by Cy+21day G-CSF did not alter the general distribution (**d**) or perivascular localization (**e**) of Tomato^{+} cells in the spleens of *Tcf21*[cre/ER]; *R26*[tdTomato] mice as compared to normal mice (Fig. 2a and 2d). **f, g,** Tomato expression was undetectable in the bone marrow of *Tcf21*[cre/ER]; *R26*[tdTomato] mice after Cy +G-CSF treatment irrespective of whether the bone marrow was analyzed by whole-mount imaging (**f**) or flow cytometry (**g**). **h, i,** EMH induced by Cy+G-CSF did not significantly

change the frequency (**h**) or perivascular localization (**i**, arrows) of Tomato^{+} cells in the livers of *Tcf21^(cre/ER); R26^(tdTomato)* mice. (**d-i**, n=3 mice from 3 independent experiments)
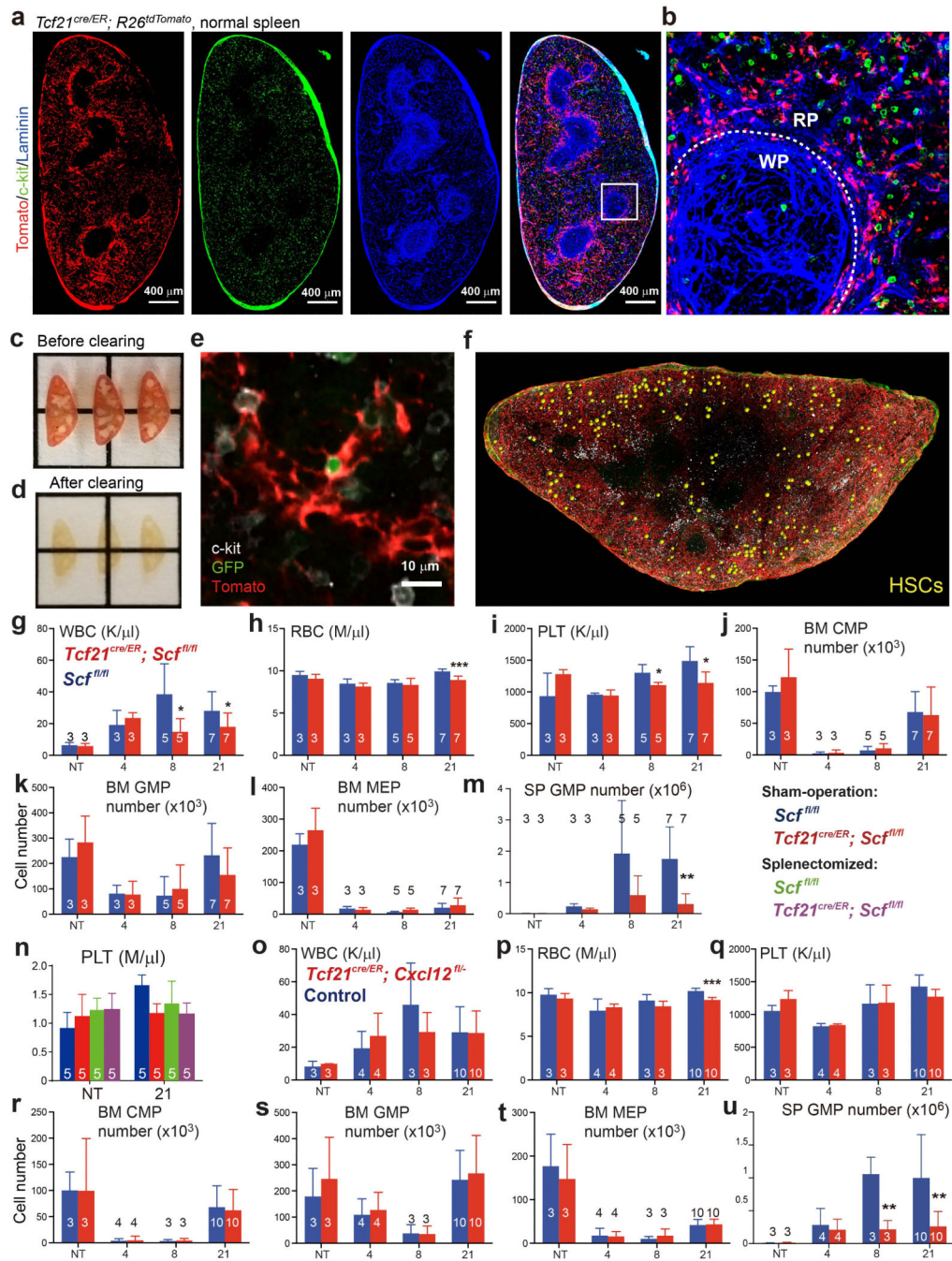
Extended Data Figure 3. Deep imaging of HSCs in the spleen; deletion of *Scf* or *Cxcl12* from *Tcf21*-expressing stromal cells in the spleen reduced peripheral blood cell counts but did not affect bone marrow haematopoiesis

a, b, The vast majority of c-kit[+] haematopoietic progenitors localized adjacent to *Tcf21*-expressing stromal cells in the red pulp of the normal spleen (n=3 mice from 3 independent experiments). **c, d,** 300 μm thick sections of spleen before (**c**) and after optical clearing (**d**).

e, f, Deep imaging of α-*catulin*-GFP$^+$c-kit$^+$ HSCs in cleared spleen segments from *Tcf21*$^{cre/ER}$*; R26*^{tdTomato}*; α-catulin* mice. A representative high magnification image of an α-*catulin*-GFP$^+$c-kit$^+$ HSC surrounded by Tomato$^+$ stromal cells (**e**). **f,** Low magnification view of a digitally reconstructed 300 μm thick spleen fragment with α-*Catulin*-GFP$^+$c-kit$^+$ HSCs identified by large yellow spheres. Note that actual HSCs would be smaller than the yellow spheres but would not be visible at this magnification (n=3 mice from 3 independent experiments). **g-m,** *Tcf21*$^{cre/ER}$*; Scf*$^{fl/fl}$ and *Scf*$^{fl/fl}$ control mice were treated with tamoxifen then examined a month later without further treatment (not treated, NT) or after treatment with cyclophosphamide plus 4, 8, or 21 days of G-CSF to induce EMH. Data show white blood cell (WBC) (**g**), red blood cell (RBC) (**h**), and platelet (PLT) counts (**i**), numbers of CMPs (**j**), GMPs (**k**) and MEPs (**l**) in the bone marrow and numbers of GMPs in the spleen (**m**). **n,** Platelet counts of sham-operated and splenectomized mice that were treated with Cy +21d G-CSF one month after surgery. **o-u,** *Tcf21*$^{cre/ER}$*; Cxcl12*$^{fl/-}$ mice and littermate controls (*Cxcl12*$^{fl/-}$ or *Cxcl12*$^{+/-}$) were treated with tamoxifen then examined a month later without further treatment (NT) or after treatment with cyclophosphamide plus 4, 8, or 21 days of G-CSF to induce EMH. Data show WBC (**o**), RBC (**p**), and PLT counts (**q**), numbers of CMPs (**r**), GMPs (**s**) and MEPs (**t**) in the bone marrow and numbers of GMPs in the spleen (**u**). The numbers of mice per treatment are shown in each panel. All data reflect mean±s.d. from 3 independent experiments. Two-tailed student's t-tests were used to assess statistical significance (*P<0.05, ***P<0.001).
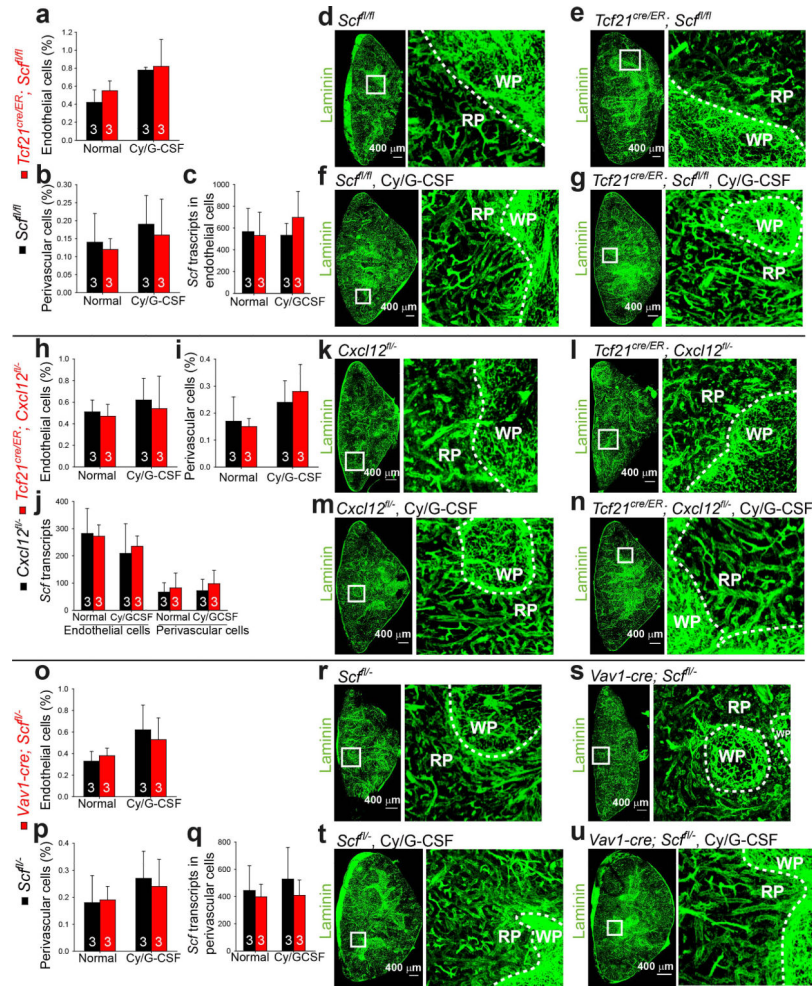
Extended Data Figure 4. Conditional deletion of *Scf* or *Cxcl12* with *Tcf21*-Cre/ER, or *Scf* with *Vav1*-Cre, does not significantly affect the frequency or morphology of stromal cells in the spleen, irrespective of EMH induction

a-g, Irrespective of whether the mice were treated with Cy+G-CSF, conditional deletion of *Scf* from *Tcf21*^{+} cells did not significantly change the frequency of VE-cadherin^{+} endothelial cells (**a**) or PDGFRβ[+] perivascular stromal cells (**b**), *Scf* transcript levels in endothelial cells (**c**), or the morphology or density of blood vessels in the spleen (**d-g**). **h-n,** Irrespective of whether the mice were treated with Cy+G-CSF, conditional deletion of *Cxcl12* from *Tcf21*^{+} cells did not significantly change the frequency of VE-cadherin^{+} endothelial cells (**h**) or PDGFRβ[+] perivascular stromal cells (**i**), *Scf* transcript levels in endothelial cells or perivascular stromal cells (**j**), or the morphology or density of blood vessels in the spleen (**k-n**). **o-u,** Irrespective of whether the mice were treated with Cy+G-CSF, conditional deletion of *Scf* from *Vav1*^{+} cells did not significantly change the frequency of VE-cadherin^{+} endothelial cells (**o**) or PDGFRβ[+] perivascular stromal cells (**p**), *Scf* transcript levels in perivascular stromal cells (**q**), or the morphology or density of blood vessels in the spleen (**r-u**). *Scf* transcript levels in flow cytometrically isolated cells were normalized to *β-actin* and then compared to whole spleen cells (**c**, **j** and **q**). The data reflect

mean±s.d. from 3 mice/genotype/condition in 3 independent experiments. Two-tailed student's t-tests were used to assess statistical significance.
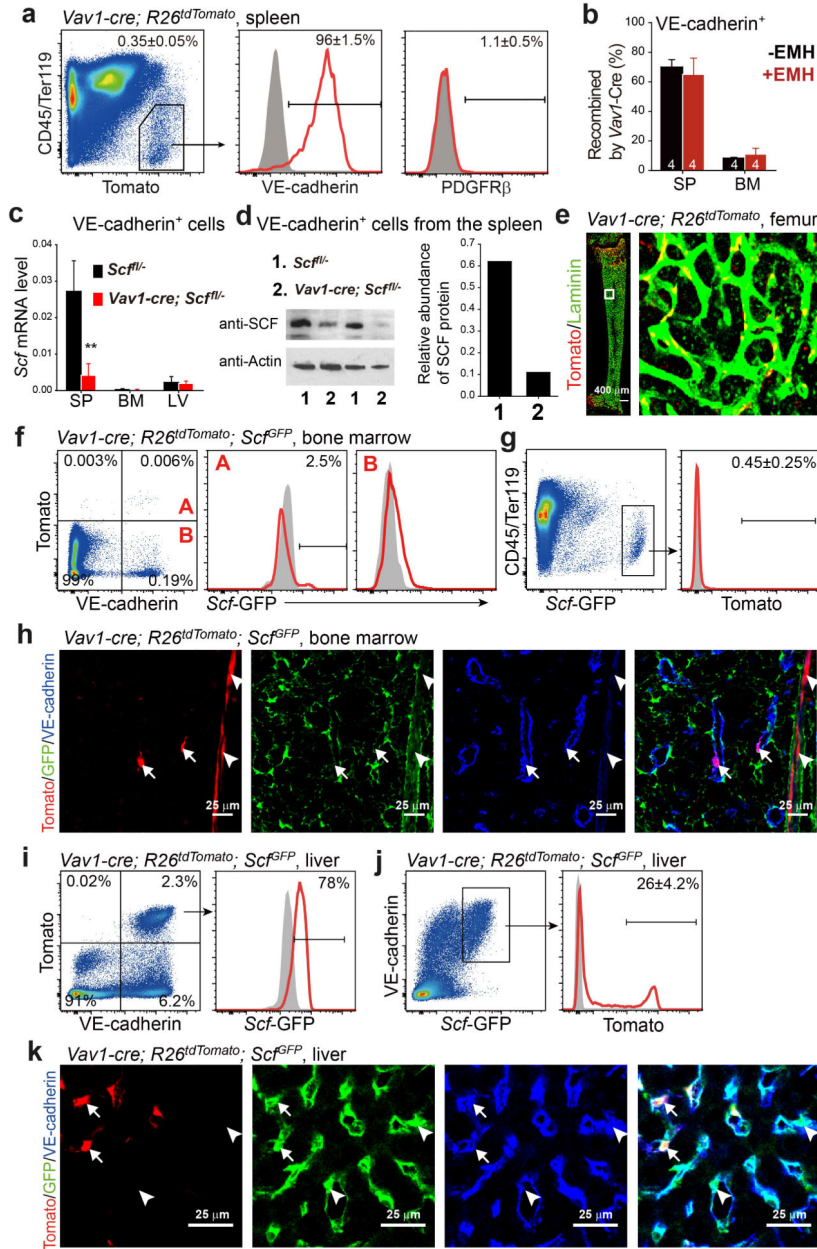
Extended Data Figure 5. *Vav1*-Cre recombines efficiently and specifically in spleen endothelial cells but poorly in bone marrow or liver endothelial cells

a, Tomato^high CD45⁻Ter119⁻ cells in *Vav1-cre; tdTomato* mice were uniformly positive for VE-cadherin and negative for PDGFRβ (n=3 mice from 3 independent experiments). **b,** *Vav1*-Cre recombined in most spleen endothelial cells but in few bone marrow endothelial cells, irrespective of Cy+G-CSF treatment (+EMH). **c,** *Scf* transcript levels were significantly reduced in endothelial cells from the spleen but not from bone marrow or liver in *Vav1-cre; Scf^fl/−* mice as compared to *Scf^fl/−* mice. The *Scf* transcript level was

normalized to *β-actin*. **d,** Western-blot showed lower SCF protein levels in splenic endothelial cells from *Vav1-cre; Scf*$^{fl/-}$ mice as compared to *Scf*$^{fl/-}$ mice. SCF abundance was assessed relative to Actin by Image J software (n=3 mice/genotype from 3 independent experiments). **e-h,** In the bone marrow *Vav1*-Cre recombined in a minority of endothelial cells, including some sinusoidal (arrows in **h**) and some arteriolar (arrowheads in **h**) endothelial cells, that expressed little *Scf*-GFP by flow cytometry (**f, g**). The data reflect mean±s.d. from 3 mice/genotype in 3 independent experiments. **i-k,** *Vav1*-Cre recombined inefficiently in liver endothelial cells. Most Tomato$^+$ cells in the liver of *Vav1-cre; R26*^{tdTomato}; *Scf*^{GFP} mice were VE-cadherin$^+$ and *Scf*-GFP$^+$ (**i**, arrows in **k**) but these cells accounted for only 26±4.2% of *Scf*-GFP$^+$ cells by flow cytometry (**i, j**) and confocal microscopy (**k**, n=3 mice from 3 independent experiments). Two-tailed student's t-tests were used to assess statistical significance.
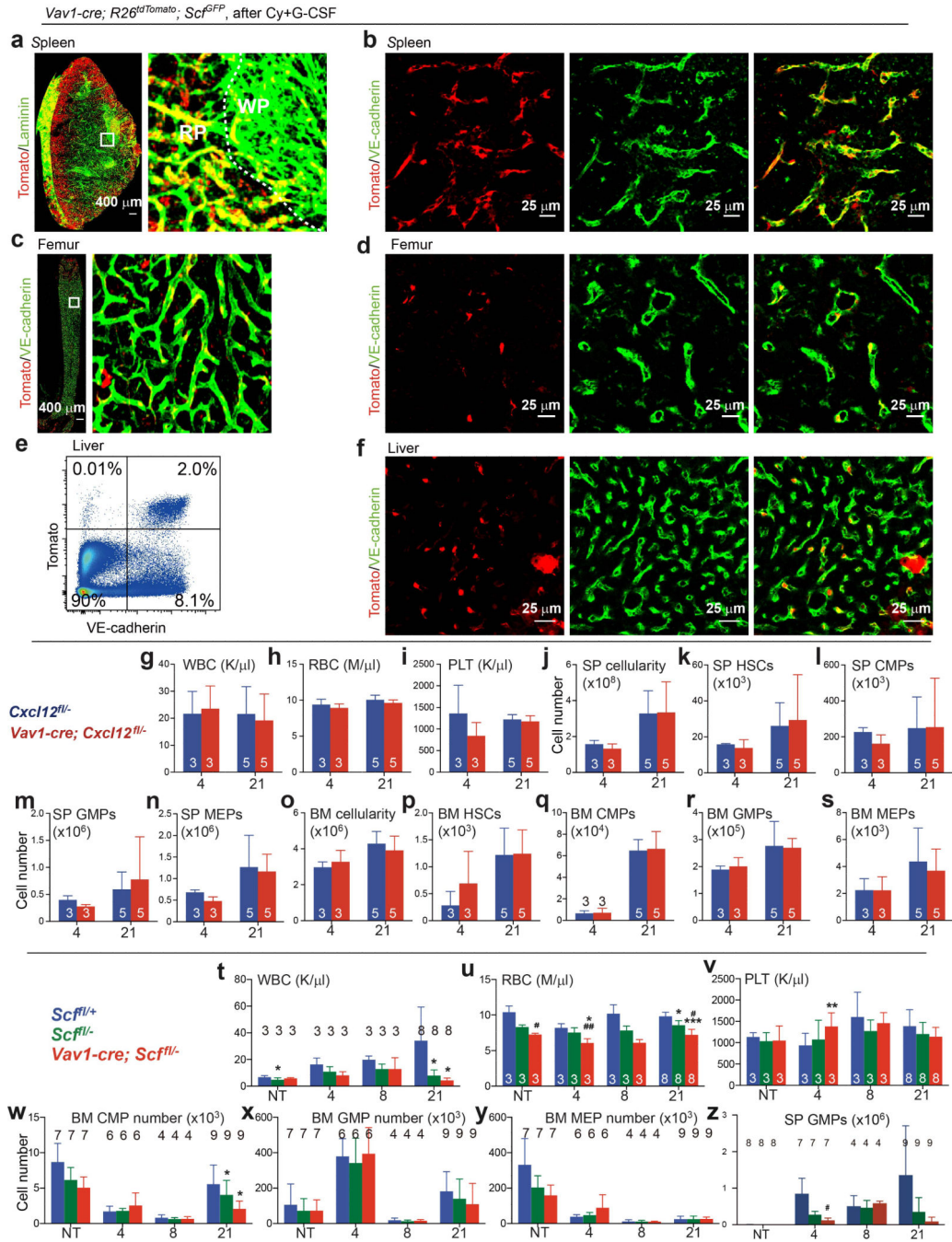
Extended Data Figure 6. EMH induced by Cy+G-CSF does not significantly change the recombination pattern of *Vav1*-Cre in the spleen, bone marrow, or liver but deletion of *Scf* from endothelial cells in spleens with EMH reduces blood cell counts without affecting bone marrow haematopoiesis

a, b, After EMH induced by Cy+21d G-CSF, *Vav1*-Cre-recombined cells were predominantly in the red pulp (**a**) and co-localized with VE-cadherin^{+} cells (**b**) in the spleen, **c-f,** After EMH induced by Cy+21d G-CSF, *Vav1*-Cre-recombined cells remained rare in the bone marrow (**c, d**) and liver (**e, f**, n=3 mice from 3 independent experiments). **g-s,** *Vav1-cre; Cxcl12^{fl/−}* mice and *Cxcl12^{fl/−}* controls were treated with Cy+4-21d G-CSF to induce EMH.

Data show WBC (**g**), RBC (**h**), and platelet (**i**) counts, spleen cellularity (**j**) and numbers of HSCs (**k**), CMPs (**l**), GMPs (**m**) and MEPs (**n**) in the spleen as well as bone marrow cellularity (**o**), and numbers of HSCs (**p**), CMPs (**q**), GMPs (**r**) and MEPs (**s**) in one femur and one tibia. The data represent mean mean±s.d. from 3 (4d) and 5 (21d) independent experiments. The number of mice/treatment is indicated on each bar. Two-tailed student's t-tests were used to assess statistical significance. **t-z,** *Vav1-cre; Scf*$^{fl/-}$ mice and *Scf*$^{fl/+}$, *Scf*$^{fl/-}$ controls were treated with Cy+4-21d G-CSF to induce EMH. Data show WBC (**t**), RBC (**u**), and platelet (PLT) (**v**) counts, numbers of CMPs (**w**), GMPs (**x**) and MEPs (**y**) in the bone marrow as well as numbers of GMPs in the spleen (**z**). Note that after 21 days of G-CSF both *Scf*$^{fl/-}$ and *Vav1-cre; Scf*$^{fl/-}$ mice showed significantly lower CMP numbers relative to *Scf*$^{fl/+}$ mice but their CMP numbers were not significant different from each other (**w**), indicating that CMP numbers in the bone marrow were not influenced by *Scf* deletion from spleen endothelial cells. The data represent mean±s.d. from 3 (NT), 3 (4d), 3 (8d), and 8 (21d) independent experiments. The number of mice/treatment is indicated on each bar. The statistical significance of differences among genotypes was assessed using Repeated Measures one-way ANOVAs with Greenhouse-Geisser correction and Tukey's multiple comparison tests with individual variances computed for each comparison. * indicates statistical significance relative to *Scf*$^{fl/+}$ controls. # indicates statistical significance between *Scf*$^{fl/-}$ and *Vav1-cre; Scf*$^{fl/-}$ (* or # P<0.05, ** or ## P<0.01).
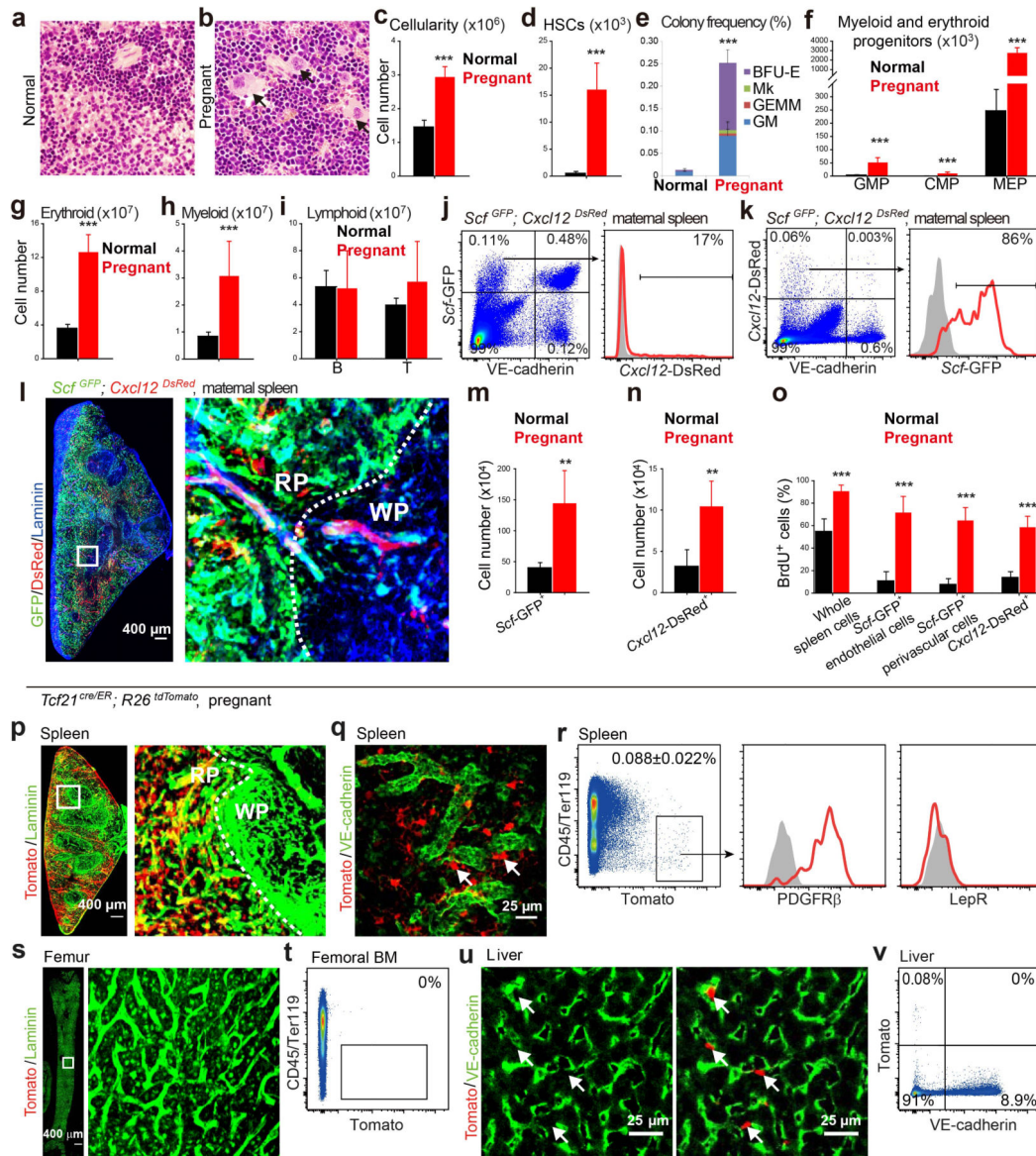
Extended Data Figure 7. Pregnancy induces EMH and the proliferation of endothelial cells and stromal cells in the spleen without significantly changing the recombination pattern of *Tcf21*-Cre/ER in the spleen, bone marrow, or liver

Pregnant female mice were at gestation day 18.5. **a, b,** H&E staining showed increased haematopoiesis in the spleens of pregnant mice (**b**) as evidenced by the presence of megakaryocytes (arrows; n=3 mice/condition from 3 independent experiments). **c-i,** Pregnancy significantly increased spleen cellularity (**c**), as well as the numbers of HSCs (**d**), myeloid and erythroid progenitors (**e, f**), Ter119^{+} erythroid cells (**g**) and Gr-1^{+}Mac-1^{+} myeloid cells (**h**) in the spleen but not the number of B220^{+} or CD3^{+} lymphoid cells (**i**). **j, k,** During pregnancy *Scf*-GFP was expressed by VE-cadherin^{+} endothelial cells and VE-cadherin^{−} stromal cells (**j**) while *Cxcl12*-DsRed was expressed by a subset of the VE-cadherin[−]*Scf*-GFP^{+} stromal cells (**j, k**). **l,** Whole-mount imaging of a thick spleen section from a pregnant *Scf*[GFP]; *Cxcl12*[DsRed] mouse (representative images from 3 mice in 3 independent experiments). **m, n,** In the spleen, the numbers of *Scf*-GFP^{+} cells (**m**) and

Cxcl12-DsRed^{+} cells (**n**) significantly increased upon bleeding. **o,** Endothelial and stromal cells in the spleen proliferated after bleeding. BrdU was administered to *Scf*[GFP] mice or *Cxcl12*[DsRed] mice for 18 days, beginning in pregnant mice after the plug was observed. The number of mice per treatment is indicated on each bar. Each panel shows mean±s.d. from three independent experiments. Two-tailed student's t-tests were used to assess statistical significance (**P<0.01, ***P<0.001). **p-r,** Pregnancy did not alter the general distribution (**p**), perivascular localization (**q**) or surface marker expression (**r**, PDGFRβ[+] and LepR[−]) of Tomato^{+} cells in the spleens of *Tcf21*[cre/ER]; *R26*[tdTomato] mice. **s, t,** Tomato expression remained undetectable in the bone marrow of pregnant *Tcf21*[cre/ER]; *R26*[tdTomato] mice. **u, v,** During pregnancy *Tcf21*-Cre/ER recombined in rare perivascular cells in the liver. (**p-v,** n=3 mice/genotype from 3 independent experiments)
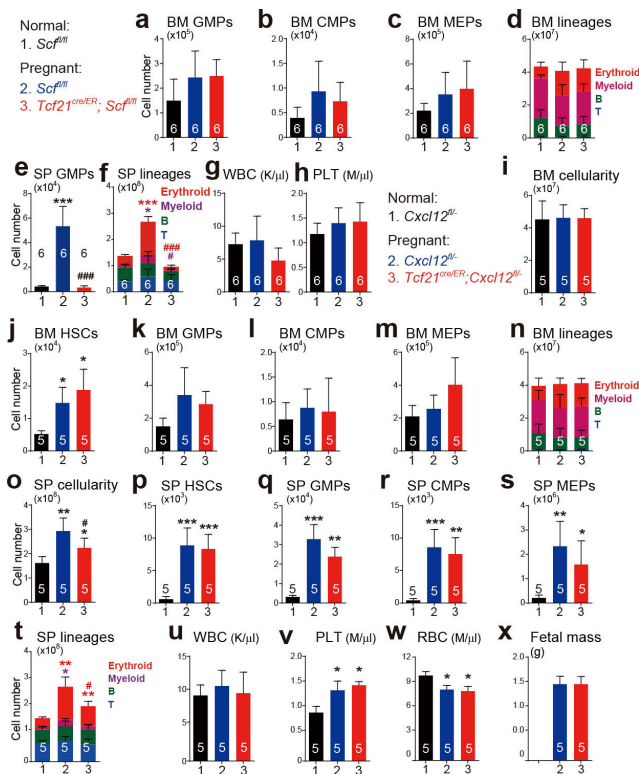
Extended Data Figure 8. Conditional deletion of *Cxcl12* from *Tcf21*^{+} stromal cells impairs EMH in the spleens of pregnant mice without significantly affecting bone marrow haematopoiesis
4 to 6 month-old female mice that had been treated with tamoxifen at least two month before were mated with normal wild-type males. Normal females and pregnant females at gestation day 18.5 were analyzed. **a-d,** Conditional deletion of *Scf* from *Tcf21*^{+} cells did not significantly affect the numbers of GMPs (**a**), CMPs (**b**), MEPs (**c**), Ter119^{+} (erythroid), Gr-1^{+}Mac-1^{+} (myeloid), CD3^{+} (T) and B220^{+} (B) cells (**d**) in one femur or one tibia. **e, f,** Conditional deletion of *Scf* from *Tcf21*^{+} cells significantly reduced GMPs (**e**), Ter119^{+} erythrocytes and Gr-1^{+}Mac-1^{+} myeloid cells (**f**) in the spleen. **g, h,** Conditional deletion of *Scf* from *Tcf21*^{+} cells did not significantly affect WBC (**g**) or platelet counts (**h**). **i-n,** Conditional deletion of *Cxcl12* from *Tcf21*^{+} cells did not significantly affect bone marrow cellularity (**i**), or the numbers of HSCs (**j**), GMPs (**k**) CMPs (**l**), MEPs (**m**), Ter119^{+}

(erythroid), Gr-1$^+$Mac-1$^+$ (myeloid), CD3$^+$ (T) and B220$^+$ (B) cells (**n**) in the bone marrow. **o-w**, Spleen cellularity (**o**) and numbers of HSCs (**p**), GMPs (**q**), CMPs (**r**), MEPs (**s**), Ter119$^+$ (erythroid), Gr-1$^+$Mac-1$^+$ (myeloid), CD3$^+$ (T) and B220$^+$ (B) cells (**t**) in the spleen and WBC (**u**), platelet (**v**) and RBC counts (**w**) in the blood. **x**, Conditional deletion of *Cxcl12* from *Tcf21*$^+$ cells in the spleens of pregnant mothers did not significantly affect fetal mass. The numbers of mice per treatment are shown in each bar within each panel. Each panel shows mean±s.d. from 3 independent experiments. The statistical significance of differences among genotypes was assessed using a Repeated Measures one-way ANOVA with Greenhouse-Geisser correction along with Tukey's multiple comparison tests with individual variances (**a-w**). The statistical significance of differences in panel **x** was assessed using a two-way ANOVA. * indicates statistical significance relative to normal mice; # indicates statistical significance between *Scf* mutant mice and control mice after bleeding (* or # P<0.05, ** or ## P<0.01, *** P<0.001).
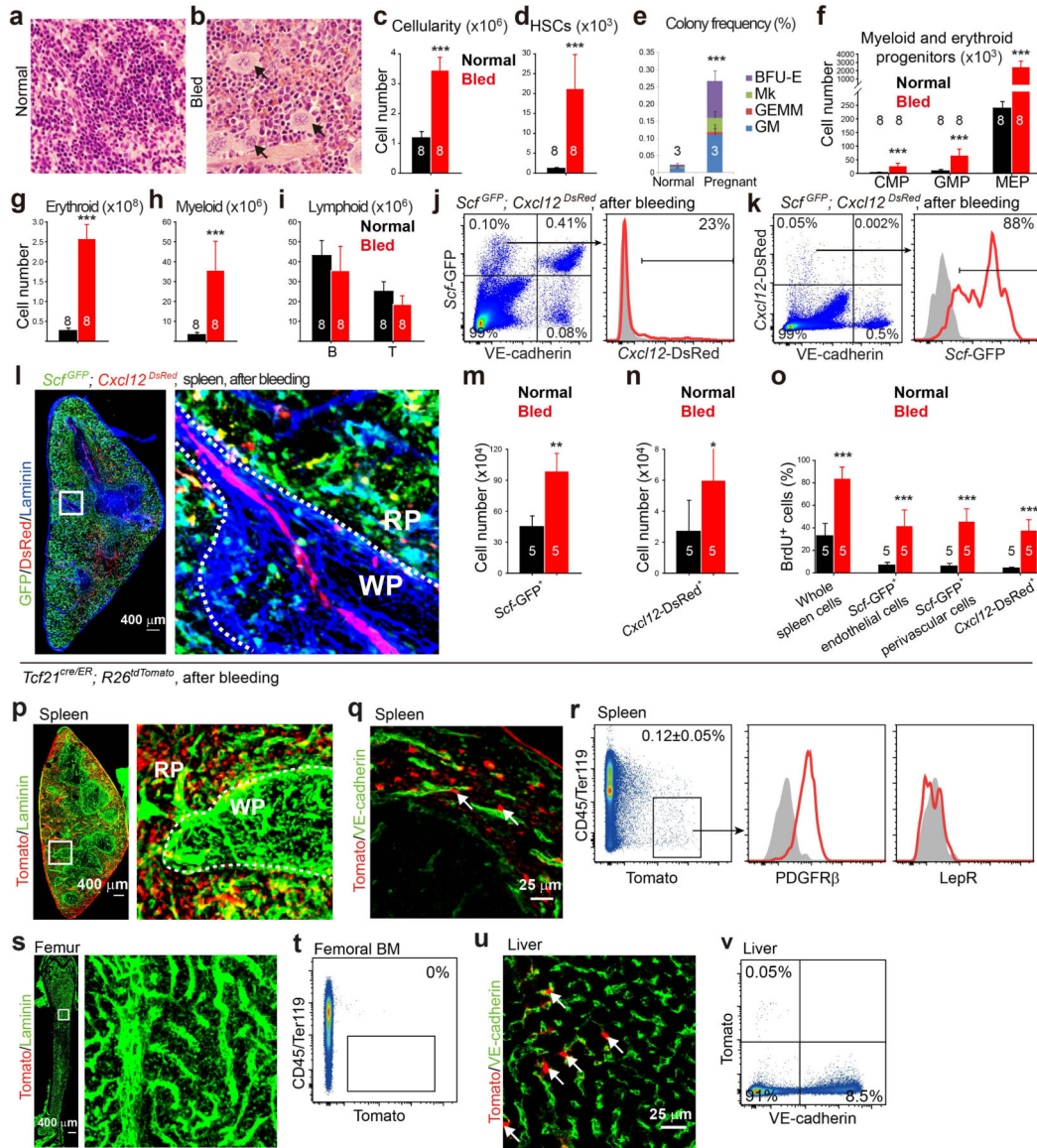
Extended Data Figure 9. Bleeding induces EMH and the proliferation of endothelial cells and stromal cells in the spleen without significantly changing the recombination pattern of *Tcf21*-Cre/ER in the spleen, bone marrow, or liver

a, b, H&E staining showed an increase in haematopoiesis in the spleen after repeated bleeding (**b**, bled) as evidenced by the presence of megakaryocytes (arrows; n=3 mice/condition from 3 independent experiments). **c-i,** Bleeding significantly increased spleen cellularity (**c**), as well as the numbers of HSCs (**d**), myeloid and erythroid progenitors (**e, f**), and the numbers of Ter119^{+} erythroid cells (**g**) and Gr-1^{+}Mac-1^{+} myeloid cells (**h**) in the spleen but not the number of B220^{+} or CD3^{+} lymphoid cells (**i**). **j, k,** After EMH induced by bleeding, *Scf*-GFP was expressed by VE-cadherin^{+} endothelial cells and VE-cadherin^{−} stromal cells (**j**) while *Cxcl12*-DsRed was expressed by a subset of the VE-cadherin[−]*Scf*-GFP^{+} stromal cells (**j, k**). **l,** Whole-mount imaging a thick spleen section from a *Scf*[GFP]; *Cxcl12*[DsRed] mouse after bleeding (representative images from 3 mice in 3 independent experiments). **m, n,** The numbers of *Scf*-GFP^{+} cells (**m**) and *Cxcl12*-DsRed^{+} cells (**n**)

significantly increased upon bleeding. **o,** Endothelial and stromal cells in the spleen proliferated after bleeding. BrdU was administered to Scf^{GFP} mice or $Cxcl12^{DsRed}$ mice for 15 days beginning after the first bleeding. The numbers of mice per treatment are shown in each bar in each panel. Each panel shows mean±s.d. from three independent experiments. Two-tailed student's t-tests were used to assess statistical significance (**P<0.01, ***P<0.001). **p-r,** Bleeding did not alter the general distribution (**p**), perivascular localization (**q**) or surface marker expression (**r**, PDGFRβ$^+$ and LepR$^-$) of Tomato$^+$ cells in the spleens of $Tcf21^{cre/ER}$; $R26^{tdTomato}$ mice. **s, t,** Tomato expression remained undetectable in bone marrow from $Tcf21^{cre/ER}$; $R26^{tdTomato}$ mice after bleeding. **u, v,** After bleeding $Tcf21$-Cre/ER recombined in only rare perivascular cells in the liver (**p-v**, n=3 mice/genotype from 3 independent experiments).
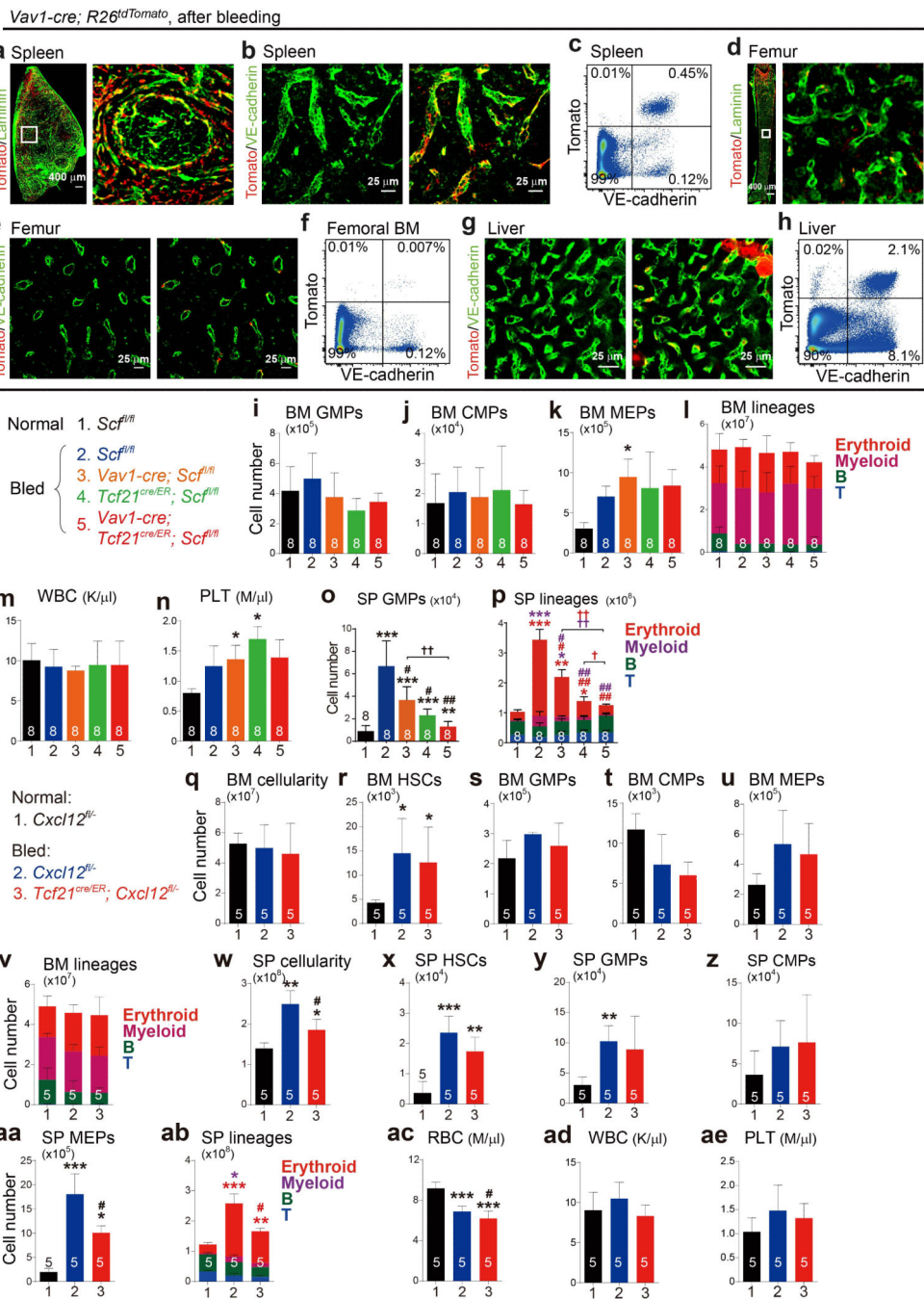
Extended Data Figure 10. Blood loss does not significantly change the recombination pattern of *Vav1*-Cre in the spleen, bone marrow, or liver; conditional deletion of *Cxcl12* from *Tcf21*^{+} spleen stromal cells in bled mice impairs EMH in the spleen without significantly affecting bone marrow haematopoiesis

4-6 month-old mice with the indicated genetic backgrounds were repeatedly bled over a two week period. **a-h,** After EMH induced by blood loss, *Vav1*-Cre recombined efficiently in VE-cadherin^{+} endothelial cells in the red pulp of the spleen (**a-c**) but poorly in the bone marrow (**d-f**) and liver (**g, h**), similar to what we observed under normal conditions (see Fig. 4a-4c and Extended Data Fig. 5b) (**a-h**, n=3 mice from 3 independent experiments). **i-n,**

Conditional deletion of *Scf* from *Tcf21*^{+} and/or *Vav1*^{+} spleen cells did not significantly affect the numbers of GMPs (**i**), CMPs (**j**), MEPs (**k**), Ter119^{+} (erythroid), Gr-1^{+}Mac-1^{+} (myeloid), CD3^{+} (T) and B220^{+} (B) cells (**l**) in the bone marrow or WBC (**m**) or platelet counts in the blood (**n**). **o, p,** Conditional deletion of *Scf* from *Tcf21*^{+} and/or *Vav1*^{+} spleen cells significantly reduced GMPs (**o**), Ter119^{+} erythrocytes and Gr-1^{+}Mac-1^{+} myeloid cells (**p**) in the spleen. (**i-p**, Data represent mean±s.d. from 3 independent experiments) **q-v,** Conditional deletion of *Cxcl12* from *Tcf21*^{+} spleen cells did not significantly affect bone marrow cellularity (**q**), or the numbers of HSCs (**r**), GMPs (**s**) CMPs (**t**), MEPs (**u**), Ter119^{+} (erythroid), Gr-1^{+}Mac-1^{+} (myeloid), CD3^{+} (T) and B220^{+} (B) cells (**v**) in one femur and one tibia from bled mice. **w-ab**, Conditional deletion of *Cxcl12* from *Tcf21*^{+} spleen cells significantly reduced spleen cellularity (**w**), and the numbers of MEPs (**aa**) and erythroid cells (**ab**) in the spleens of bled mice. Conditional deletion of *Cxcl12* from *Tcf21*^{+} spleen cells did not significantly affect the numbers of HSCs (**x**), GMPs (**y**), or CMPs (**z**) in the spleens of bled mice. **ac-ae**, Conditional deletion of *Cxcl12* from *Tcf21*^{+} spleen cells significantly reduced RBC (**ac**) but not WBC (**ad**) or platelet counts (**ae**) in the blood of mice that had been repeatedly bled. The data in **q-ae** represent mean±s.d. from 3 independent experiments. The numbers of mice per treatment are shown in each bar in each panel. Statistical significance of differences among genotypes was assessed using a Repeated Measures one-way ANOVA with Greenhouse-Geisser correction along with Tukey's multiple comparison tests with individual variances. * indicates statistical significance relative to normal mice; # indicates statistical significance between *Scf* mutant mice and control mice after bleeding (* or # $P<0.05$, ** or ## $P<0.01$, *** $P<0.001$).

Extended Data Table 1

Genes that are significantly (>8-fold and P<0.015) more highly expressed by *Scf*-GFP+ stromal cells in spleen as compared to bone marrow.

Gene	Gene name	Unigene	Spleen *Scf*-GFP+	BM *Scf*-GFP+	Fold change
Coch	Coagulation factor C homolog	Mm.21325	12.1±0.3	6.6±0.0	45.4
Ccl21a	Chemokine (C-C motif) ligand 21A	Mm.458815	12.5±0.1	7.1±0.4	41.1
Acta2	Actin, alpha 2, smooth muscle, aorta	Mm.213025	11.9±0.3	6.7±0.1	35.2
Cxcl13	Chemokine (C-X-C motif) ligand 13	Mm.10116	11.8±0.3	6.8±0.2	30.3
Tcf21	Transcription factor 21	Mm.16497	11.3±0.6	6.6±0.0	25.9
Clca1	Chloride channel calcium activated 1	Mm.454553	11.1±0.3	6.6±0.0	22.5
Ifi27l2a	Interferon, alpha-inducible protein 27 like 2A	Mm.271275	11.3±0.2	7.2±0.4	16.6
Pln	Phospholamban	Mm.34145	10.7±0.1	6.6±0.0	16.3
Parm1	Prostate androgen-regulated mucin-like 1	Mm.5002	10.8±0.3	6.8±0.1	16
Fn1	Fibronectin 1	Mm.193099	10.7±0.4	6.8±0.2	14.9
Col14a1	Collagen, type XIV, alpha 1	Mm.297859	10.4±0.2	6.7±0.1	12.6
Nr4a1	Nuclear receptor subfamily 4, group A, 1	Mm.119	10.5±0.6	7.0±0.3	11.2
Agtr1a	Angiotensin II receptor, type 1a	Mm.35062	10.7±0.7	7.3±0.6	11
Fos	FBJ osteosarcoma oncogene	Mm.246513	11.4±0.4	8.0±0.4	10.7
Atp1b2	ATPase, Na+/K+ transporter, beta 2	Mm.235204	10.6±0.2	7.2±0.2	10.6
Tnxb	Tenascin XB	Mm.290527	9.9±0.5	6.6±0.0	9.5
Myh11	Myosin, heavy polypeptide 11, smooth muscle	Mm.250705	10.7±0.7	7.5±0.2	9.4
Hspb1	Heat shock protein 1	Mm. 13849	10.8±0.7	7.6±0.2	9.3
Clca2	Chloride channel calcium activated 2	Mm.20897	9.8±0.4	6.6±0.0	8.8
Tagln	Transgelin	Mm.283283	10.4±0.5	7.3±0.9	8.6
Nr2f2	Nuclear receptor subfamily 2, group F, 2	Mm.158143	10.7±0.3	7.6±0.3	8.5
Mustn1	Musculoskeletal, embryonic nuclear protein 1	Mm.220895	10.8±0.5	7.7±0.7	8.2
Aspn	Asporin	Mm.383216	9.7±0.6	6.6±0.0	8.2
Sparcl1	SPARC-like 1	Mm.29027	12.1±0.1	9.1±0.4	8.1

Data show mean±s.d. for log2 transformed expression values (n=3 independent samples/cell population). Maximal background expression was considered to be 6.6 (log2(100)); all expression values below this threshold were set to 6.6 for purposes of calculating fold-change. Two-tailed Student's t-tests were used to assess statistical significance. Data for bone marrow *Scf*-GFP+ stromal cells are from [19].

Supplementary Material

Refer to Web version on PubMed Central for supplementary material.

Acknowledgements

REFERENCE

1. Abdel-Wahab OI, Levine RL. Primary myelofibrosis: update on definition, pathogenesis, and treatment. Annual Review Medicine. 2009; 60:233–45.

2. Cheshier SH, Prohaska SS, Weissman IL. The effect of bleeding on hematopoietic stem cell cycling and self-renewal. Stem Cells Dev. 2007; 16:707–17. [PubMed: 17999593]

3. Bennett M, Pinkerton PH, Cudkowicz G, Bannerman RM. Hemopoietic progenitor cells in marrow and spleen of mice with hereditary iron deficiency anemia. Blood. 1968; 32:908–21. [PubMed: 4881978]

4. Nakada D, et al. Oestrogen increases haematopoietic stem-cell self-renewal in females and during pregnancy. Nature. 2014; 505:555–8. [PubMed: 24451543]

5. Fowler JH, Nash DJ. Erythropoiesis in the spleen and bone marrow of the pregnant mouse. Developmental Biology. 1968; 18:331–53. [PubMed: 5752783]

6. Baldridge MT, King KY, Boles NC, Weksberg DC, Goodell MA. Quiescent haematopoietic stem cells are activated by IFN-gamma in response to chronic infection. Nature. 2010; 465:793–7. [PubMed: 20535209]

7. Burberry A, et al. Infection mobilizes hematopoietic stem cells through cooperative NOD-like receptor and Toll-like receptor signaling. Cell Host Microbe. 2014; 15:779–91. [PubMed: 24882704]

8. Morrison SJ, Wright DE, Weissman IL. Cyclophosphamide/granulocyte colony- stimulating factor induces hematopoietic stem cells to proliferate prior to mobilization. Proc Natl Acad Sci U S A. 1997; 94:1908–13. [PubMed: 9050878]

9. Dutta P, et al. Myocardial infarction accelerates atherosclerosis. Nature. 2012; 487:325–9. [PubMed: 22763456]

10. Lowell CA, Niwa M, Soriano P, Varmus HE. Deficiency of the Hck and Src tyrosine kinases results in extreme levels of extramedullary hematopoiesis. Blood. 1996; 87:1780–92. [PubMed: 8634424]

11. Freedman MH, Saunders EF. Hematopoiesis in the human spleen. American Journal of Hematology. 1981; 11:271–5. [PubMed: 7053225]

12. Tavassoli M, Weiss L. An electron microscopic study of spleen in myelofibrosis with myeloid metaplasia. Blood. 1973; 42:267–79. [PubMed: 4793115]

13. Johns JL, Christopher MM. Extramedullary hematopoiesis: a new look at the underlying stem cell niche, theories of development, and occurrence in animals. Veterinary Pathology. 2012; 49:508–23. [PubMed: 22262354]

14. Kiel MJ, Yilmaz OH, Iwashita T, Terhorst C, Morrison SJ. SLAM family receptors distinguish hematopoietic stem and progenitor cells and reveal endothelial niches for stem cells. Cell. 2005; 121:1109–21. [PubMed: 15989959]

15. Miwa Y, et al. Up-regulated expression of CXCL12 in human spleens with extramedullary haematopoiesis. Pathology. 2013; 45:408–16. [PubMed: 23619587]

16. Chow A, et al. CD169(+) macrophages provide a niche promoting erythropoiesis under homeostasis and stress. Nature Medicine. 2013; 19:429–36.

17. Morita Y, et al. Functional characterization of hematopoietic stem cells in the spleen. Experimental Hematology. 2011; 39:351–359. e3. [PubMed: 21185906]

18. Ding L, Morrison SJ. Haematopoietic stem cells and early lymphoid progenitors occupy distinct bone marrow niches. Nature. 2013; 495:231–5. [PubMed: 23434755]

19. Ding L, Saunders TL, Enikolopov G, Morrison SJ. Endothelial and perivascular cells maintain haematopoietic stem cells. Nature. 2012; 481:457–62. [PubMed: 22281595]

20. Zhou BO, Yue R, Murphy MM, Peyer JG, Morrison SJ. Leptin-receptor-expressing mesenchymal stromal cells represent the main source of bone formed by adult bone marrow. Cell Stem Cell. 2014; 15:154–68. [PubMed: 24953181]

21. Acharya A, Baek ST, Banfi S, Eskiocak B, Tallquist MD. Efficient inducible Cre- mediated recombination in Tcf21 cell lineages in the heart and kidney. Genesis. 2011; 49:870–7. [PubMed: 21432986]

22. Acar M, et al. Deep imaging of bone marrow shows non-dividing stem cells are perisinusoidal. Nature. 2015 In Press.

23. Akashi K, Traver D, Miyamoto T, Weissman IL. A clonogenic common myeloid progenitor that gives rise to all myeloid lineages. Nature. 2000; 404:193–7. [PubMed: 10724173]

24. de Boer J, et al. Transgenic mice with hematopoietic and lymphoid specific expression of Cre. European Journal of Immunology. 2003; 33:314–25. [PubMed: 12548562]

25. Sugiyama T, Kohara H, Noda M, Nagasawa T. Maintenance of the hematopoietic stem cell pool by CXCL12-CXCR4 chemokine signaling in bone marrow stromal cell niches. Immunity. 2006; 25:977–88. [PubMed: 17174120]

26. Madisen L, et al. A robust and high-throughput Cre reporting and characterization system for the whole mouse brain. Nature Neuroscience. 2010; 13:133–40. [PubMed: 20023653]

27. DeFalco J, et al. Virus-assisted mapping of neural inputs to a feeding center in the hypothalamus. Science. 2001; 291:2608–13. [PubMed: 11283374]

28. Becker K, Jahrling N, Saghafi S, Dodt HU. Immunostaining, dehydration, and clearing of mouse embryos for ultramicroscopy. Cold Spring Harbor protocols. 2013; 2013:743–4. [PubMed: 23906920]

29. Irizarry RA, et al. Exploration, normalization, and summaries of high density oligonucleotide array probe level data. Biostatistics. 2003; 4:249–64. [PubMed: 12925520]

30. Cesta MF. Normal structure, function, and histology of the spleen. Toxicol Pathol. 2006; 34:455–65. [PubMed: 17067939]

31. Tronche F, et al. Disruption of the glucocorticoid receptor gene in the nervous system results in reduced anxiety. Nat Genet. 1999; 23:99–103. [PubMed: 10471508]

32. Zhu X, Bergles DE, Nishiyama A. NG2 cells generate both oligodendrocytes and gray matter astrocytes. Development. 2008; 135:145–57. [PubMed: 18045844]

33. Zhu X, et al. Age-dependent fate and lineage restriction of single NG2 cells. Development. 2011; 138:745–53. [PubMed: 21266410]

34. Logan M, et al. Expression of Cre Recombinase in the developing mouse limb bud driven by a Prxl enhancer. Genesis. 2002; 33:77–80. [PubMed: 12112875]

35. Rivers LE, et al. PDGFRA/NG2 glia generate myelinating oligodendrocytes and piriform projection neurons in adult mice. Nat Neurosci. 2008; 11:1392–401. [PubMed: 18849983]

36. Cuttler AS, et al. Characterization of Pdgfrb-Cre transgenic mice reveals reduction of ROSA26 reporter activity in remodeling arteries. Genesis. 2011; 49:673–80. [PubMed: 21557454]

37. Holtwick R, et al. Smooth muscle-selective deletion of guanylyl cyclase-A prevents the acute but not chronic effects of ANP on blood pressure. Proc Natl Acad Sci U S A. 2002; 99:7142–7. [PubMed: 11997476]

38. Xin HB, Deng KY, Rishniw M, Ji G, Kotlikoff MI. Smooth muscle expression of Cre recombinase and eGFP in transgenic mice. Physiol Genomics. 2002; 10:211–5. [PubMed: 12209023]

39. Wendling O, Bornert JM, Chambon P, Metzger D. Efficient temporally-controlled targeted mutagenesis in smooth muscle cells of the adult mouse. Genesis. 2009; 47:14–8. [PubMed: 18942088]
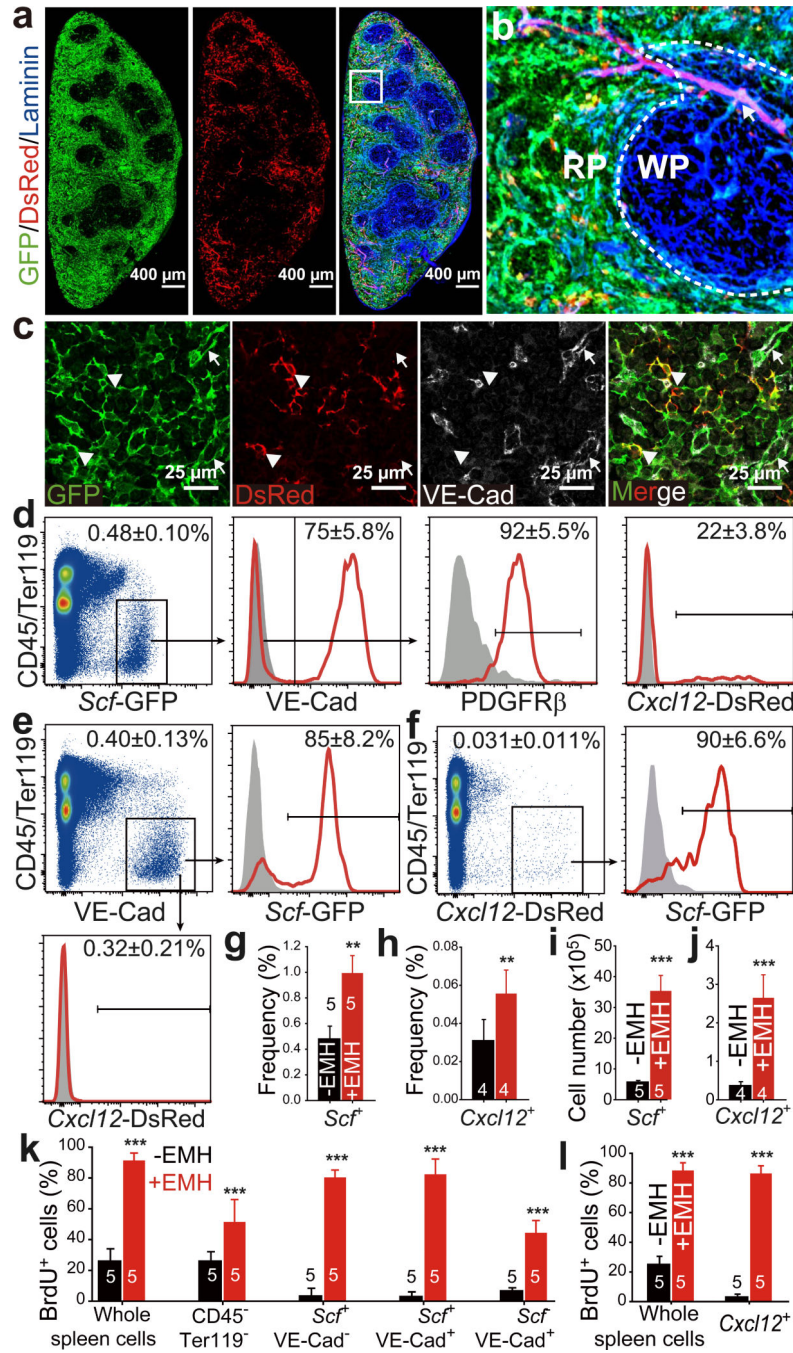
Figure 1. Endothelial cells and perivascular stromal cells in the red pulp express *Scf* and *Cxcl12* and proliferate upon induction of EMH

a, b, *Scf*-GFP and *Cxcl12*-DsRed were mainly expressed by stromal cells in the red pulp (RP) of normal spleens. (**b**) High-magnification view of the boxed area in (**a**). Dashed lines depict the boundary between white pulp (WP) and red pulp (RP). Arrow indicates central arteriole in the WP, around which rare stromal cells expressed *Cxcl12*-DsRed. **c,** Splenic RP from *Scf^GFP*; *Cxcl12^DsRed* mice had VE-cadherin^+ endothelial cells (arrows) that expressed *Scf*-GFP and VE-cadherin^− stromal cells (arrowheads) that expressed *Scf*-GFP and

sometimes *Cxcl12*-DsRed. **d-f,** Flow cytometric analysis of enzymatically dissociated spleen cells from *Scf^{GFP}; Cxcl12^{DsRed}* mice. *Scf*-GFP was expressed by VE-cadherin^{+} endothelial cells and PDGFRβ[+]VE-cadherin^{−} stromal cells, a subset of which also expressed *Cxcl12*-DsRed (**d**). Most VE-cadherin^{+} endothelial cells were positive for *Scf*-GFP but negative for *Cxcl12*-DsRed (**e**). Most *Cxcl12*-DsRed^{+} cells were positive for *Scf*-GFP (**f**). Data in **a-f** represent mean±s.d. from 3 mice from 3 independent experiments. **g-l,** The frequencies and absolute numbers of *Scf*-GFP^{+} cells (**g, i**) and *Cxcl12*-DsRed^{+} cells (**h, j**) significantly increased upon induction of EMH by Cy+21d G-CSF (+EMH). **k, l,** BrdU was co-administered to *Scf^{GFP}* (**k**) or *Cxcl12^{DsRed}* mice (**l**) along with G-CSF for 7 days after cyclophosphamide treatment. Data represent mean±s.d. from 3 independent experiments. The numbers of mice per treatment are shown on the bars in panels **g-l**. Two-tailed student's t-tests were used to assess statistical significance (**P<0.01, ***P<0.001).
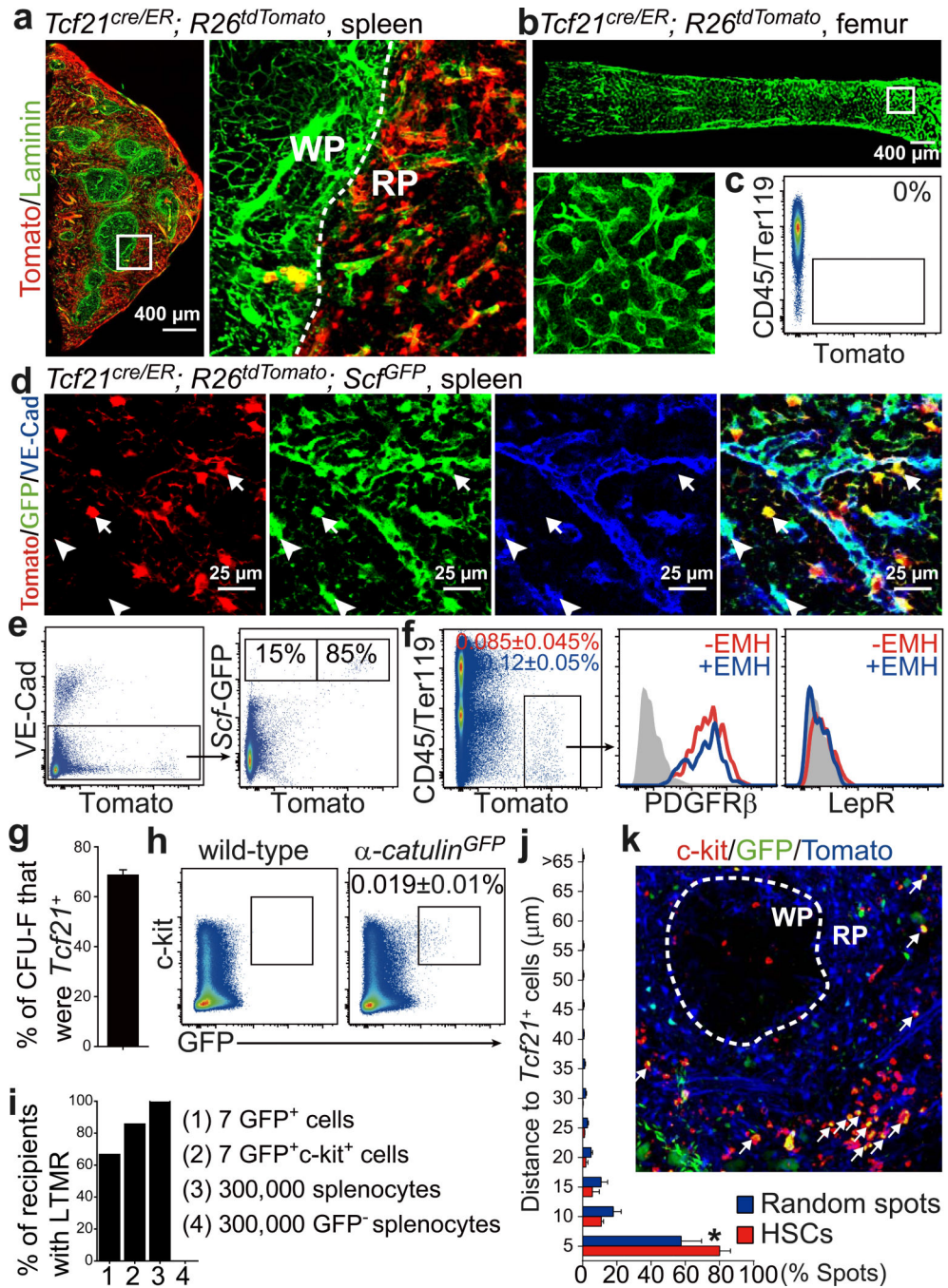
Figure 2. During EMH most HSCs localize adjacent to *Tcf21*^{+} stromal cells in the red pulp

a, Tamoxifen-treated adult *Tcf21*[cre/ER]*; R26*[tdTomato] mice exhibited widespread Tomato expression by perivascular stromal cells in the red pulp (RP). **b, c,** No Tomato expression in bone marrow from tamoxifen-treated *Tcf21*[cre/ER]*; R26*[tdTomato] mice. **d, e,** Most *Scf*-GFP[+]VE-cadherin^{−} stromal cells were Tomato^{+} (arrows) whereas *Scf*-GFP^{+}VE-cadherin^{+} endothelial cells were Tomato^{−} (arrowhead). **f,** Tomato^{+}CD45^{−}Ter119^{−} stromal cells from enzymatically dissociated spleen from *Tcf21*[cre/ER]*; R26*[tdTomato] mice were positive for PDGFRβ but negative for LepR, irrespective of EMH induction by Cy+G-CSF. **g,**

Percentage of all CFU-F colonies formed by enzymatically dissociated $Tcf21^{cre/ER}$; $R26^{tdTomato}$ spleen cells that were Tomato$^+$. Macrophage colonies were excluded by staining with anti-CD45 antibody. **h,** α-catulin-GFP$^+$c-kit$^+$ HSCs represented 0.019±0.01% of dissociated spleen cells in α-catulin^{GFP} mice with EMH. **i,** α-catulin-GFP$^+$c-kit$^+$ splenocytes were highly enriched for long-term multilineage reconstituting (LTMR) HSCs. **j, k,** Deep imaging of α-catulin-GFP$^+$c-kit$^+$ HSCs (arrows in **k**) in optically cleared spleen from a $Tcf21^{cre/ER}$; $R26^{tdTomato}$; α-catulin^{GFP} mouse with EMH induced by Cy+21d G-CSF. The distance from α-catulin-GFP$^+$c-kit$^+$ HSCs or random spots to Tomato$^+$ stromal cells (**j;** *p<0.05 by two-tailed student's t-test). α-catulin-GFP$^+$c-kit$^+$ HSCs were exclusively in the RP (**k;** see Extended Data Fig. 3f for a low magnification view). All data reflect mean±s.d. from 3 mice in 3 independent experiments.
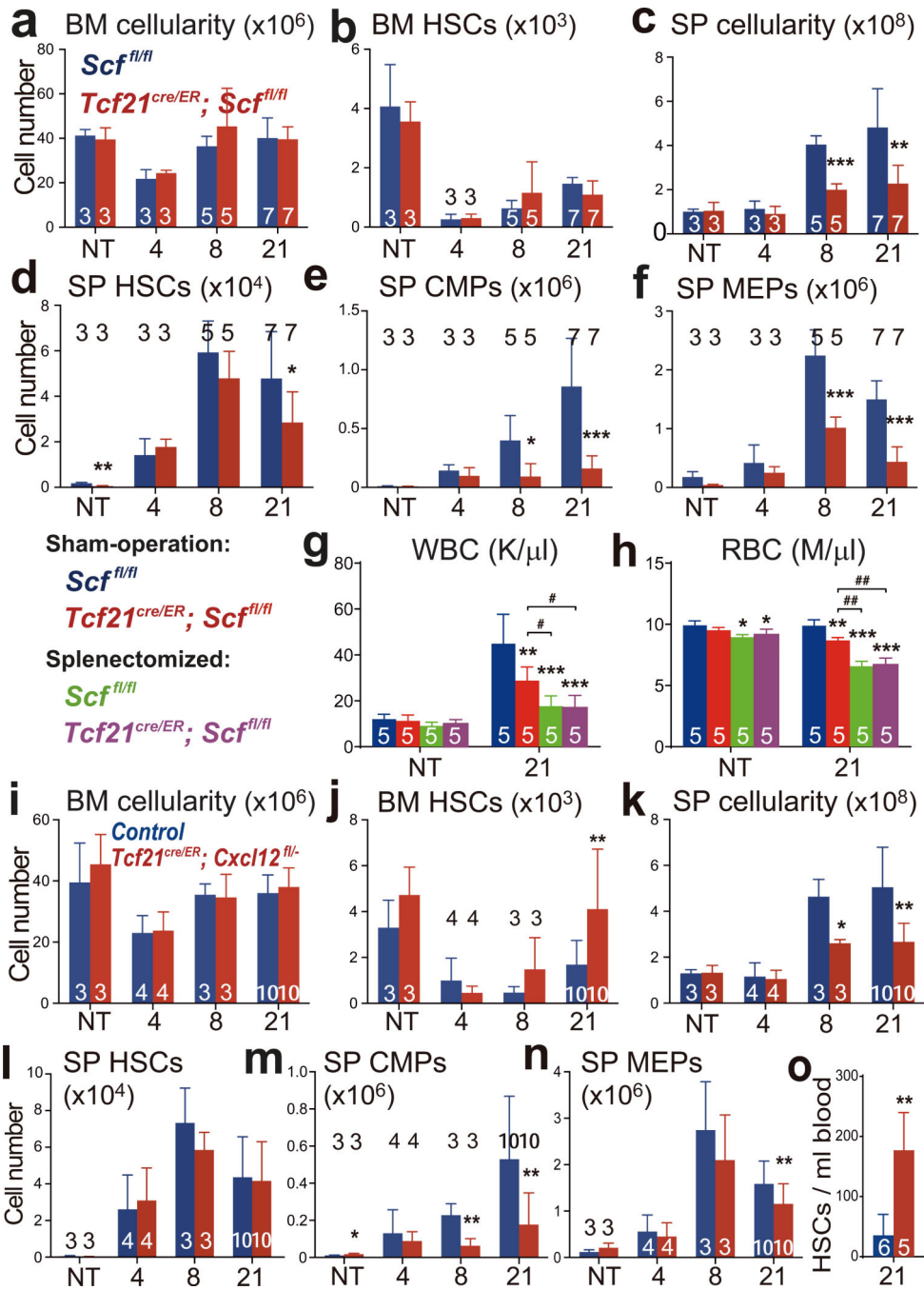
Figure 3. *Tcf21*-expressing stromal cells are an important source of *Scf* and *Cxcl12* for EMH in the spleen

a-f, $Tcf21^{cre/ER}$; $Scf^{fl/fl}$ and $Scf^{fl/fl}$ control mice were treated with tamoxifen then examined a month later either under normal conditions (not treated, NT) or after treatment with cyclophosphamide plus 4, 8, or 21 days of G-CSF to induce EMH. The number of bone marrow cells (**a**) and bone marrow $CD150^+CD48^-LSK$ HSCs (**b**) in one femur plus one tibia as well as spleen cellularity (**c**), and the numbers of HSCs (**d**), common myeloid progenitors (CMPs, **e**) and megakaryocyte/erythroid progenitors (MEPs, **f**), in the spleen. **g, h,** Sham-operated and splenectomized mice were treated with Cy+21d G-CSF one month after

surgery: white blood cell (WBC; **g**) and red blood cell (RBC; **h**) counts. **i-o,** *Tcf21^{cre/ER};
Cxcl12^{fl/−}* and *Cxcl12^{+/−}* or *Cxcl12^{fl/−}* control mice were treated with tamoxifen then
examined a month later either under normal conditions (NT) or after treatment with
cyclophosphamide plus 4, 8, or 21 days of G-CSF to induce EMH. The number of bone
marrow cells (**i**) and bone marrow HSCs (**j**) in one femur plus one tibia as well as spleen
cellularity (**k**), numbers of HSCs (**l**), CMPs (**m**) and MEPs (**n**) in the spleen. **o,** Number of
HSCs per ml of blood in tamoxifen-treated control and *Tcf21^{cre/ER}; Cxcl12^{fl/−}* mice after Cy
+21d G-CSF. The numbers of mice per treatment are shown in each bar in each panel. All
panels reflect mean±s.d. from three independent experiments. * indicates statistical
significance relative to sham-operated *Scf^{fl/fl}* mice while # indicates statistical significance
among other treatments (* or # P<0.05, ** or ## P<0.01, *** P<0.001).
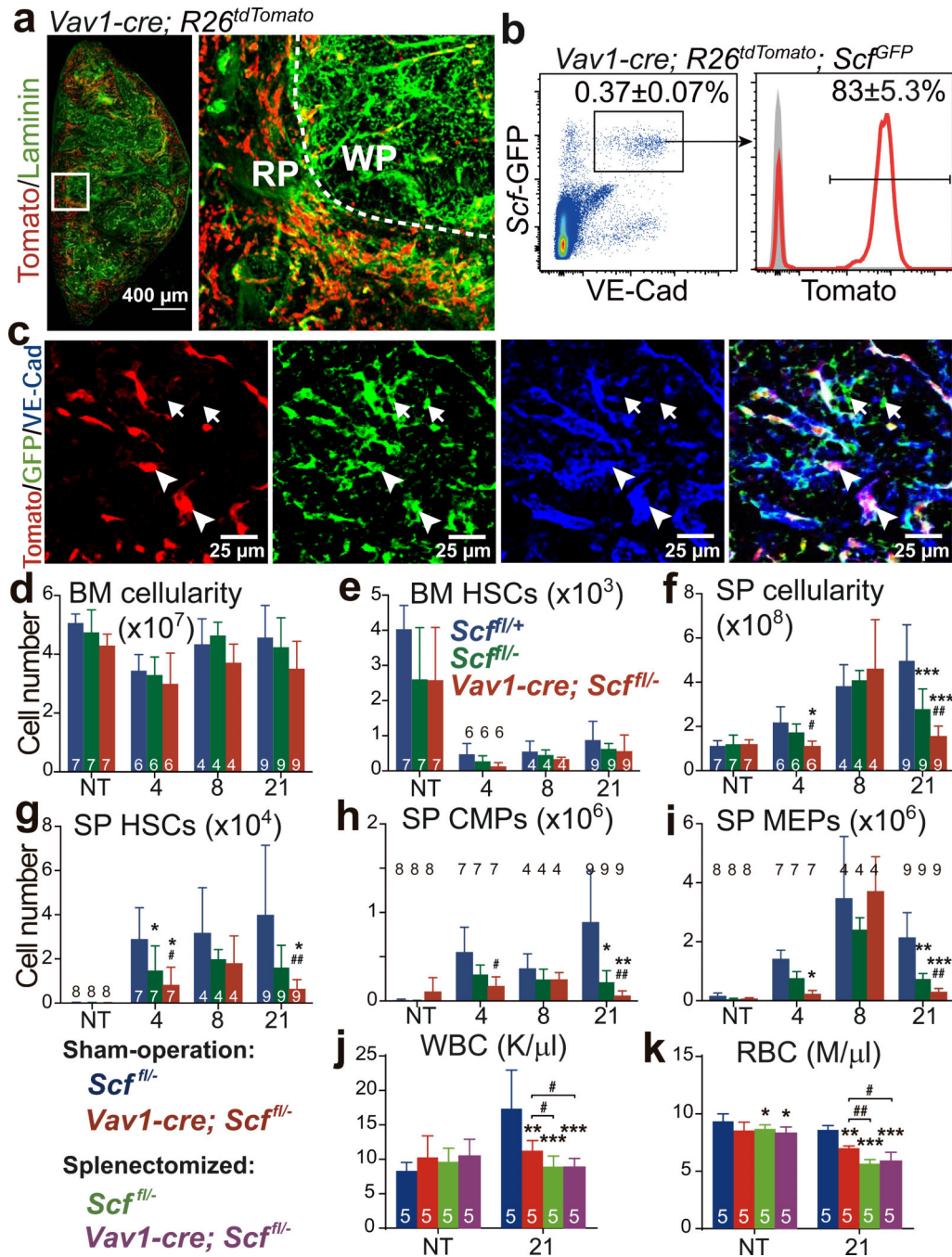
Figure 4. Endothelial cells are an important source of *Scf* for EMH in the spleen

a, *Vav1-cre; R26^{tdTomato}* mice exhibited vascular Tomato expression throughout the splenic red pulp (RP). Tomato was also expressed by haematopoietic cells in these mice but levels of Tomato expression in endothelial cells were ~10-100 fold higher than in haematopoietic cells. Therefore short-exposure images showed mainly Tomato fluorescence in endothelial cells. **b, c,** *Vav1*-Cre recombined in VE-cadherin[+]*Scf*-GFP^{+} endothelial cells (arrowheads in **c**) but not in VE-cadherin[−]*Scf*-GFP[+] perivascular stromal cells (arrows in **c**). **d-i,** *Vav1-cre; Scf^{fl/−}* mice and *Scf^{fl/+}*, *Scf^{fl/−}* controls were not treated (NT) or treated with

cyclophosphamide plus 4, 8, or 21 days of G-CSF to induce EMH. Data show the number of bone marrow cells (**d**) and bone marrow HSCs (**e**) in one femur plus one tibia as well as spleen cellularity (**f**) and the numbers of HSCs (**g**), CMPs (**h**) and MEPs (**i**) in the spleen. **j, k,** WBC (**j**) and RBC (**k**) counts in splenectomized and sham-operated mice before and after Cy+21day G-CSF treatment. The numbers of mice per treatment are shown in the bars in each panel. All data reflect mean±s.d. from 3 (**a-c**; **j, k**) or 6 (**d-i**) independent experiments. * indicates statistical significance relative to $Scf^{fl/+}$ mice while # indicates statistical significance between $Scf^{fl/-}$ and $Vav1\text{-}cre; Scf^{fl/-}$ mice (**d-i**); * indicates statistical significance relative to sham-operated $Scf^{fl/-}$ mice while # indicates statistical significance between other treatments (**j, k**) (* or # P<0.05, ** or ## P<0.01, *** P<0.001).
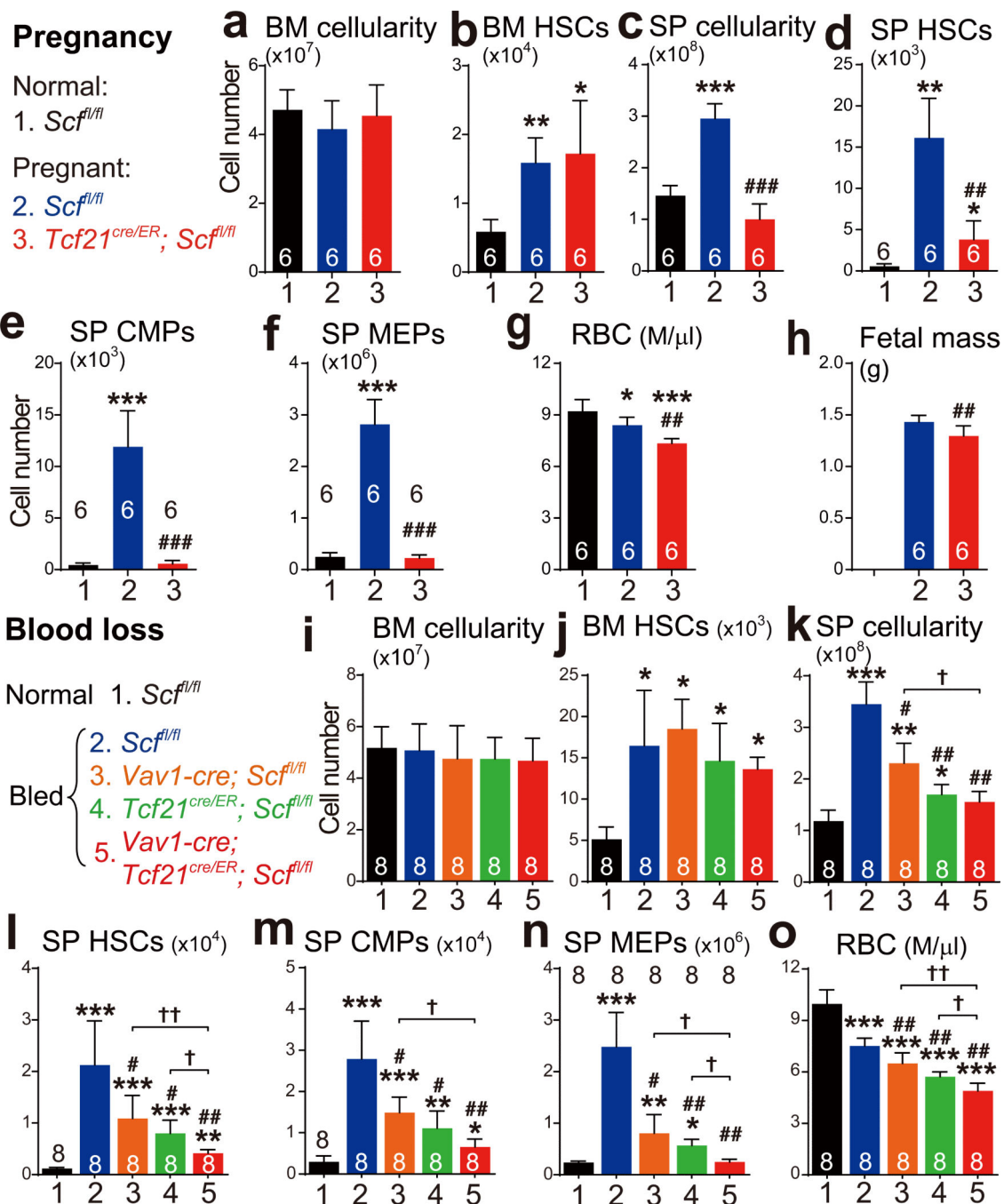
Figure 5. *Scf* from endothelial cells and *Tcf21*^{+} stromal cells is necessary for splenic EMH and adequate erythropoiesis after bleeding or during pregnancy

a-h, 4-6 month-old female mice that had been treated with tamoxifen at least two months earlier were mated with normal wild-type males. Normal females and pregnant females at gestation day 18.5 were analyzed: the number of bone marrow cells (**a**) and bone marrow HSCs (**b**) in one femur plus one tibia as well as spleen cellularity (**c**), and the numbers of HSCs (**d**), CMPs (**e**) and MEPs (**f**) in the spleen. RBC counts (**g**) and fetal mass (**h**). **i-o,** 4-6 month-old mice with the indicated genetic backgrounds were repeatedly bled over a two

week period then analyzed: the number of bone marrow cells (**i**) and bone marrow HSCs (**j** in one femur plus one tibia as well as spleen cellularity (**k**), and the numbers of HSCs (**l**), CMPs (**m**) and MEPs (**n**) in the spleen. RBC counts (**o**). The numbers of mice per treatment are shown in each bar of each panel. All data reflect mean±s.d. from four (**a-h**) or three (**i-o**) independent experiments. * indicates statistical significance relative to normal mice; # indicates statistical significance between *Scf* mutant mice and control mice after bleeding or pregnancy; † indicate statistical significance between single mutants and compound mutants (*, # or † P<0.05, **, ## or †† P<0.01, ***or ### P<0.001).